Molecular Pharmacology Fast Forward. Published on October 19, 2010 as DOI: 10.1124/mol.110.066910
This article has not been copyedited and formatted. The final version may differ from this version.
Molecular Pharmacology Fast Forward. Published on October 19, 2010 as doi:10.1124/mol.110.066910

MOL #66910

Curcumin dually inhibits both mTOR and NF-κB pathways through a crossed PI3K/Akt/IKK signaling axis in adenoid cystic carcinoma

Zhi-Jun Sun, Gang Chen, Wei Zhang, Xiang Hu, Yang Liu, Qian Zhou, Ling-Xing Zhu, and Yi-Fang Zhao

The State Key Laboratory Breeding Base of Basic Science of Stomatology & Key Laboratory of Oral Biomedicine Ministry of Education (Z.-J.S., G.C., W.Z., X.H., Y.L., Q.Z., L.-X.Z., Y.-F.Z.); and Department of Oral and Maxillofacial Surgery, School & Hospital of Stomatology, Wuhan University, Wuhan, China (Z.-J.S., G.C., W.Z., X.H., Y.-F.Z.)

Downloaded from molpharm.aspetjournals.org at ASPET Journals on April 19, 2024

Copyright 2010 by the American Society for Pharmacology and Experimental Therapeutics.

Molecular Pharmacology Fast Forward. Published on October 19, 2010 as DOI: 10.1124/mol.110.066910
This article has not been copyedited and formatted. The final version may differ from this version.

Running title: mTOR and NF-κB pathways in adenoid cystic carcinoma

Address correspondence to: Yi-Fang Zhao, Department of Oral and Maxillofacial Surgery, School and Hospital of Stomatology, Wuhan University, Wuhan 430079, China. Phone: 86-27-87686158; Fax: 86-27-87873260; E-mail: yifang@whuss.com.

Number of text pages: 30

Number of words in Abstract: 248

Number of words in Introduction: 597

Number of words in Discussion: 1346

Number of References: 37

Number of tables: 0

Number of Figures: 7 (Color Figures: 3; Black and White Figures: 4)

Number of Supplementary Data: 1

ABBREVIATIONS: ACC, adenoid cystic carcinoma; mTOR, mammalian target of rapamycin; MAPK, mitogen-activated protein kinase; JNK, c-Jun NH_2-terminal kinase; ERK, extracellular signal-regulated kinase; NF-κB, nuclear factor-κB; IKK, IκBα kinase; PI3K, phosphatidylinositol 3-kinase; VEGF, vascular endothelial growth factor; b-FGF, basic fibroblast growth factor; G-CSF, granulocyte colony stimulating factor; PDGF, platelet-derived growth factor; IL-6, interleukin-6; MMP, matrix metalloproteinase; MVD, microvessel density; CM, conditioned medium; NSG, normal salivary gland; DMSO, dimethyl sulfoxide; PDTC, pyrrolidine dithiocarbamate; DMEM, Dulbecco's modified Eagle's medium; FBS, fetal bovine serum; PBS, phosphate-buffered saline; CAM, chick chorioallantoic membrane; TUNEL, terminal deoxynucleotidyl transferase-mediated dUTP-biotin nick end labeling.

Downloaded from molpharm.aspetjournals.org at ASPET Journals on April 19, 2024

Molecular Pharmacology Fast Forward. Published on October 19, 2010 as DOI: 10.1124/mol.110.066910
This article has not been copyedited and formatted. The final version may differ from this version.

ABSTRACT

Adenoid cystic carcinoma (ACC) is a highly malignant tumor that is generally unresponsive or only weakly responsive to the currently available antineoplastic agents. Thus novel therapeutic strategies and agents are urgently needed to treat this aggressive neoplasm. Curcumin, a component of turmeric (*Curcuma longa*), has been shown to have a diversity of anti-tumor activities. We show here that curcumin is a potent inhibitor of ACC progression *in vitro* and *in vivo*. Curcumin concentration-dependently inhibited the growth of ACC cells via induction of apoptosis. The ability of ACC cells to migrate/invade and induce angiogenesis was also significantly attenuated by curcumin, accompanied by the down-regulation of vascular endothelial growth factor (VEGF), matrix metalloproteinase-2 and -9. Moreover, our data also demonstrated that the inhibitory effects of curcumin on ACC cells were due to its dual-inhibition of both mammalian target of rapamycin (mTOR) and nuclear factor-κB (NF-κB) pathways through a crossed PI3K/Akt/IKK signaling axis. Most importantly, curcumin effectively prevented the *in vivo* growth and angiogenesis of ACC xenografts in nude mice, as revealed by the induction of cell apoptosis and reduction of microvessel density (MVD) in tumor tissues. Additionally, we further assessed the nature activation status of both mTOR and NF-κB pathways in ACC tissues, and confirmed the concurrent high activation of these two pathways in ACC for the first time. Taken together, our findings suggest that further clinical investigation is warranted to apply curcumin as a novel chemotherapeutic regimen for ACC due to its dual-suppression of both mTOR and NF-κB pathways.

Downloaded from molpharm.aspetjournals.org at ASPET Journals on April 19, 2024

Molecular Pharmacology Fast Forward. Published on October 19, 2010 as DOI: 10.1124/mol.110.066910
This article has not been copyedited and formatted. The final version may differ from this version.

Introduction

Adenoid cystic carcinoma (ACC), a highly aggressive neoplasm mostly occurring in the salivary gland and breast (Persson et al., 2009), accounts for around 22% of all salivary gland malignancies, and about 1% of all head and neck malignancies (Hotte et al., 2005). After curative surgery, radiotherapy as well as chemotherapy, the disease-specific survival at 10 years for patients with ACC remains to be 29% to 40% (Fordice et al., 1999). Most deaths from salivary ACC are caused by local recurrence and distant metastasis those are resistant to conventional therapy. Therefore, effective agents with minimal untoward side effects are urgently needed to control the malignant progression of ACC.

Curcumin [1,7-bis(4-hydroxy-3-methoxyphenyl)-1–6-heptadine-3,5-dione; $C_{21}H_{20}O_6$], a natural polyphenol derived from the spice turmeric (*Curcuma longa*), is one such agent that has been demonstrated to be nontoxic to humans (Lao et al., 2006). Extensive researches over several decades have shown that curcumin possesses anti-inflammatory, anti-oxidant, anti-viral and anti-infectious activities (Goel et al., 2008). Furthermore, curcumin has been shown to prevent tumor initiation, promotion, and metastasis in breast, ovarian, colon, lung, and other cancers (Aggarwal et al., 2005; Li et al., 2004; Lin et al., 2007; Milacic et al., 2008; Padhye et al., 2010; Wang et al., 2008). These anti-tumor effects of curcumin seems to be closely linked to its ability to inhibit cell proliferation, induce cell apoptosis, suppress cell invasion, and reduce angiogenesis (Lev-Ari et al., 2006; Shankar et al., 2008; Yodkeeree et al., 2008; Yoysungnoen et al., 2006). Notably, this compound has entered clinical trials for certain human cancers (Anand et al., 2008; Dhillon et al., 2008) .

Extensive studies have revealed that curcumin exerts its wide range of anti-tumor effects through modulating a diversity of signaling pathways involving transcription factor nuclear factor-κB (NF-κB), IκBα kinase (IKK), phosphatidylinositol 3-kinase (PI3K), Akt, extracellular signal-regulated kinase (ERK), c-Jun NH_2-terminal kinase (JNK), p38 mitogen-activated protein kinase (p38 MAPK), and others (Aggarwal et al., 2006; Chen and Zheng, 2008; Kunnumakkara et al., 2007). Among those implicated, however, NF-κB is generally regarded as the most potent target (Li et al., 2004; Lin et al., 2007). Curcumin has the capacity to suppress NF-κB activation

Downloaded from molpharm.aspetjournals.org at ASPET Journals on April 19, 2024

Molecular Pharmacology Fast Forward. Published on October 19, 2010 as DOI: 10.1124/mol.110.066910
This article has not been copyedited and formatted. The final version may differ from this version.

through inhibition of IKK, Akt-dependently or Akt-independently (Kunnumakkara et al., 2008; Lin et al., 2007; Wang et al., 2008). In this regard, curcumin has also shown to be a potent Akt-dependent inhibitor of mammalian target of rapamycin (mTOR) (Beevers et al., 2006; Li et al., 2007; Yu et al., 2008), which has been identified as a key player in tumor progression (Seeliger et al., 2007). Nevertheless, it is worthwhile to mention that mTOR can also be Akt-independently activated by the IKKβ pathway, and blockade of IKKβ is able to inactivate mTOR (Lee et al., 2008; Seeliger et al., 2007). Thus, it is plausible that curcumin, a tested inhibitor of IKKβ (Aggarwal et al., 2006; Shishodia et al., 2005), could target both IKKβ and Akt to inactivate the mTOR pathway. However, to our best knowledge, the precise crosstalk mechanisms underlying the anti-tumor activities of curcumin, especially in ACC, are still far from clear.

Here, we initially explored the role of curcumin in ACC, and found that curcumin not only significantly inhibited *in vitro* growth, migration/invasion, and angiogenesis-induction in ACC cells, but also effectively prevented the *in vivo* growth and angiogenesis of ACC-M tumors in mice, relating with the dual-inhibition of both mTOR and NF-κB pathways through a crossed PI3K/Akt/IKK signaling axis. Further, we assessed the nature activation status of both mTOR and NF-κB pathways in ACC tissues, and confirmed the concurrent high activation levels of these two pathways in ACC for the first time.

Downloaded from molpharm.aspetjournals.org at ASPET Journals on April 19, 2024

Molecular Pharmacology Fast Forward. Published on October 19, 2010 as DOI: 10.1124/mol.110.066910
This article has not been copyedited and formatted. The final version may differ from this version.

Materials and Methods

Reagents and Plasmids. Curcumin (>98% pure), dimethyl sulfoxide (DMSO), PI3K inhibitor LY294002, NF-κB inhibitor pyrrolidine dithiocarbamate (PDTC), IKK inhibitor PS1145, mTOR inhibitor rapamycin, Hoechst 33258, propidium iodide (PI), acridine orange, and ribonuclease (RNase) were purchased from Sigma-Aldrich (St. Louis, MO). Dulbecco's modified Eagle's medium (DMEM), fetal bovine serum (FBS), penicillin, and streptomycin were obtained from GIBCO (Carlsbad, CA). Primary antibodies against human phospho-PI3K p85 (Tyr458), PI3K, phospho-Akt (Ser473), Akt, NF-κB p65, IκB-α, phospho-IKK-α/β (Ser176/180), IKK-α/β, phospho-mTOR (Ser2448), mTOR, phospho-ERK (Thr202/Tyr204), ERK, phospho-p38 (Thr180/Tyr182), p38, Phospho-JNK (Thr183/Tyr185), JNK, phospho-S6 (Ser235/236), Bax, Bcl-2, and cleaved poly (ADP-ribose) polymerase (PARP) were purchased from Cell Signaling Technology (Danvers, MA). Primary antibodies against mouse CD31, Histone H2A, and β-actin were purchased from Santa Cruz Biotechnology, Inc. (Santa Cruz, CA). The expression vectors encoding constitutively active Akt (pUSE-CA-Akt), as well as the corresponding empty vectors (pUSE) were kindly provided by Dr. Michael Robinson (University of Pennsylvania, USA).

Patients, Immunohistochemistry and Double-labeling Immunofluorescence Histochemistry. Fifty pathologically confirmed human ACC specimens, with corresponding 6 pericancerous normal salivary gland (NSG) tissues were collected at Hospital of Stomatology, Wuhan University. All specimens were fixed in buffered 4% paraformaldehyde and embedded in paraffin. The procedures were performed in accordance with the National Institutes of Health guidelines regarding the use of human tissues. The study was approved from the review board of the Ethics Committee of Hospital of Stomatology, Wuhan University. The immunohistochemical and double-labeling immunofluorescence histochemical analyses were performed according to our previous procedures (Sun et al., 2010a), as described in Supplementary Materials and Methods.

Downloaded from molpharm.aspetjournals.org at ASPET Journals on April 19, 2024

Molecular Pharmacology Fast Forward. Published on October 19, 2010 as DOI: 10.1124/mol.110.066910
This article has not been copyedited and formatted. The final version may differ from this version.

Cell Culture and Conditional Medium Collection. The high (ACC-M) and low (ACC-2) metastasis cell lines of human ACC (Guan et al., 1997) and human endothelial hybridoma cell line EAhy926 were obtained from the China Center for Type Culture Collection, and maintained in DMEM supplemented with 10% FBS, 100 U/mL penicillin, and 100 μg/mL streptomycin in a humidified atmosphere of 95% air and 5% CO_2 at 37 °C. Cells were serum starved for 12 h before treatment with curcumin in serum-deprived medium.

When ACC cells were grown to 70% confluence after overnight incubation, they were serum starved for 12 h and then treated with or without curcumin in serum-deprived DMEM medium as indicated. After 12 h, cells were washed thoroughly with PBS and further incubated in serum-deprived medium for another 24 h, then the cleared supernatants were collected as conditional medium (CM) and stored at -80 °C.

Transient Transfection. ACC cells seeded in 6 cm culture dishes were transfected with pUSE-CA-Akt or pUSE vector plasmids using Lipofectamine™ 2000 (Invitrogen, Carlsbad, CA) according to the manufacturer's instruction. The expression of p-Akt after the transfection was confirmed by Western blotting.

Cell Growth Analysis and Viability Measurement. Cell Titer-Glo (CTG; Promega Madison, WI) luminescent assay was performed to measure the growth curves of ACC cells. This luminescent assay determines the presence of live cells in a growing culture based on the quantitation of adenosine triphosphate released by metabolically active cells. Briefly, both ACC-2 and ACC-M cells (5000 cells/well) were seeded in a 96-well microplate (Corning Life Sciences, Lowell, MA) in a final volume of 100 μL. After overnight incubation, cells were treated with indicated concentrations of curcumin for 12, 24, 48, or 72 h. After completion of the treatment, 100 μL of CTG solution was added to each well and incubated for 20 min at room temperature in the dark. Lysate (50 μL) was transferred to a 96-well white plate (Greiner Bio-One GmbH, Frickenhausen, Germany), and then the luminescence was measured. Percent cell growth was calculated by considering 100% growth at the time of curcumin addition. Cell viability was measured by the

Downloaded from molpharm.aspetjournals.org at ASPET Journals on April 19, 2024

Molecular Pharmacology Fast Forward. Published on October 19, 2010 as DOI: 10.1124/mol.110.066910
This article has not been copyedited and formatted. The final version may differ from this version.

Vi-CELL cell viability analyzer (Beckman coulter, Fullerton, CA) under the same treatment conditions as mentioned for the CTG assay.

Determination of Apoptosis. Apoptosis induction by curcumin in ACC cells was determined according to our previous procedures (Sun et al., 2010a) as follows: (a) morphological evaluation by Hoechst staining; (b) quantitation of cytoplasmic histone-associated DNA fragments with Cell Death Detection ELISA^{PLUS} kit (Roche, Applied Science, Germany); (c) quantitative assessment of early and late apoptosis using the Annexin V-FITC/PI double-staining kit (BD Biosciences, San Jose, CA); (d) caspase-3 and -9 activity measurement by Colorimetric Caspase Activity Assay kit (BD Pharmingen); and (e) Western blot analysis for Bax/Bcl-2 ratio and PARP cleavage. See Supplementary Materials and Methods for more details.

Tumor Cell Migration and Invasion Assays. The ability of ACC-M cells to pass through Matrigel-coated filters was measured using Transwell Boyden chamber (Corning) containing a 6.5 mm diameter polycarbonate filter (pore size of 8 μm). Matrigel was diluted to 200 μg/mL and applied to the top side of the filter in cell invasion assays, whereas in cell migration assays filter was not coated. ACC-M cells treated with or without indicated concentration of curcumin for 12 h were seeded on the upper chamber at a density of 2×10^4 cells/well in 100 μL of serum-deprived medium, whereas medium with 10% FBS was applied to the lower chamber as chemoattractant. After incubation for 24 h at 37 °C, the cells in the upper surface of the membrane were carefully removed with a cotton swab, and migrated or invaded cells were fixed with methanol, stained with eosin dye, and then photographed and quantified.

Assessment of *In Vitro* and *In Vivo* ACC-induced angiogenesis. The effects of curcumin on ACC-induced angiogenesis were determined by a set of angiogenesis assays as previously described (Sun et al., 2010b), including the endothelial cell migration and capillary-like tube formation assays *in vitro*, as well as the rat aortic ring, chicken chorioallantoic membrane (CAM), and Matrigel plug assays *in vivo*. See Supplementary Materials and Methods for more details.

Downloaded from molpharm.aspetjournals.org at ASPET Journals on April 19, 2024

Molecular Pharmacology Fast Forward. Published on October 19, 2010 as DOI: 10.1124/mol.110.066910
This article has not been copyedited and formatted. The final version may differ from this version.

Semi-Quantitative Reverse Transcription-PCR. To evaluate the mRNA expression of growth factors, interleukin-6 (IL-6), and matrix metalloproteinases (MMPs) after curcumin treatment, semi-quantitative reverse transcription (RT)-PCR was performed. Total RNA was isolated with TRIzol Reagent (Invitrogen). Aliquots (1 μg) of RNA were reverse transcribed to cDNA (20 μL) with Oligo dT and AMV reverse transcriptase (Takara, Kyoto, Japan). One-fifth of the cDNA was used as a template for PCR using a PE9700 RT-PCR system (Applied Biosystems, Foster City, CA). The PCR products were electrophoresed in 2% agarose gel and visualized with ethidium bromide. The intensity of each band was analyzed densitometrically using Gene Tools software (Syngene, Cambridge, UK). See Supplementary Materials and Methods for the designed primer sequences for PCR.

ELISAs for Secretion of Growth Factors, IL-6, and MMPs. ACC-M cells were seeded in six-well plates, either untreated or treated with indicated concentrations of curcumin for 12 h. After that the cells were washed thoroughly with PBS and further incubated in serum-deprived medium for another 24 h to allow irritating factor production. Subsequently, the supernatants were collected and used to determine secretion of VEGF, basic fibroblast growth factor (bFGF), granulocyte colony stimulating factor (G-CSF), platelet-derived growth factor (PDGF), IL-6, MMP-2, and MMP-9 using commercially available kits (R&D Systems, Minneapolis, MN) according to the manufacturers' recommendations.

Double-labeling immunofluorescence analysis for cell. The indirect immunofluorescence analyses for cells were performed as previously described (Sun et al., 2010a).

Western Blot Analysis. The Western blot analysis was performed as described earlier (Sun et al., 2010a). Briefly, a total amount of 40 μg protein from each sample in different groups was denatured, separated using a 10% sodium dodecylsulfate-polyacrylamide gel electrophoresis (SDS-PAGE) and electroblotted on polyvinylidene fluoride membranes (Millipore Corporation, Billerica, MA). The immunoblots were blocked with 5% non-fat dry milk at room temperature for 1 h,

Downloaded from molpharm.aspetjournals.org at ASPET Journals on April 19, 2024

Molecular Pharmacology Fast Forward. Published on October 19, 2010 as DOI: 10.1124/mol.110.066910
This article has not been copyedited and formatted. The final version may differ from this version.

and then cultured overnight at 4 °C with the primary antibodies at dilutions recommended by the suppliers, followed by incubulation with horseradish peroxidase-conjugated secondary antibody (Pierce Chemical, Rockford, IL) for 1 h at room temperature. Then blots were developed by a SuperEnhanced chemiluminescence detection kit (Applygen Technologies Inc., Beijing, People's Republic of China).

Nude Mice Xenografts. Female BALB/c nude mice (18-20 g; 6-8 weeks of age) were purchased from the Experimental Animal Center of Wuhan University in pressurized ventilated cage according to institutional regulations. All studies were approved and supervised by Animal Care and Use Committee of Wuhan University. Exponentially growing ACC-M cells (2×10^6 in 0.2 mL medium) were inoculated subcutaneously into the flank of the mice. After 7 days, tumor-bearing mice were randomly divided into two groups, which were respectively given with curcumin (1 g/kg, p.o., daily; n=8) or corn oil (Control, 100 μL, p.o., daily; n=8) for 28 consecutive days. Tumor growth was determined by measuring the size of the tumors daily. Tumor volumes were calculated according to the formula ($width^2 \times length)/2$. The mice were euthanatized at Day 28, and the tumors were captured, photographed, and then embedded in paraffin or frozen at -80 °C for the following immunohistochemical analysis, terminal deoxynucleotidyl transferase-mediated dUTP-biotin nick end labeling (TUNEL) assay and microvessel density (MVD) detection, as described in Supplementary Materials and Methods.

Statistical Analysis. All values were expressed as mean ± SE of three independent experiments. One-way analysis of variance (ANOVA), Student-Newman-Keuls, as well as Spearman rank correlation test were used for statistical analysis. $P < 0.05$ was considered significantly different.

Downloaded from molpharm.aspetjournals.org at ASPET Journals on April 19, 2024

Molecular Pharmacology Fast Forward. Published on October 19, 2010 as DOI: 10.1124/mol.110.066910
This article has not been copyedited and formatted. The final version may differ from this version.

Results

Curcumin Inhibits the Growth of ACC Cells. As shown in Fig. 1, A and B, curcumin concentration-dependently inhibited the growth of both ACC-2 and ACC-M cells, but more prominent in ACC-M cells. An approximate 6-fold induction in the growth of ACC-M cells was noticed at 72 h in the absence of curcumin. Treatment with increased concentrations of curcumin (10, 20, and 40 μM) decreased the cell growth of ACC-M by almost 25%, 70% and 100% at 12 h, respectively (Fig. 1B). Notably, we also observed that curcumin treatment at the concentrations of 20 and 40 μM resulted in an even lower cell growth below 100% at 48 and 72 h, indicating probable cell death. We then determined the cell viability after curcumin treatment (Fig. 2, C and D). The results showed that all the tested concentrations of curcumin demonstrated no effect on ACC cell survival at 12 h, suggesting that the growth inhibition of ACC cells by curcumin at 12 h was not associated with cell death. However significant death of ACC cells at 24, 48 and 72 h was noticed when treated with 20 and 40 μM of curcumin. Thus, based on these results, we selected 12 h for curcumin treatment in the tumor cell migration/invasion, as well as angiogenesis-induction assays in order to avoid the interference from cell death. However, curcumin treatment for 24 h was used in the other experiments.

Curcumin Induces Apoptosis of ACC Cells. To determine whether the cytotoxicity exerted by curcumin was due to apoptosis induction, morphological observation was firstly performed microscopically. As shown in Fig. 2A, after exposure to 20 μM curcumin for 24 h, several apoptotic morphological features such as apoptotic bodies, cell shrinkage and chromatin condensation were observed in both ACC-2 and ACC-M cells by Hoechst 33258 staining assays. Then we quantitatively assessed the DNA fragmentation using the Cell Death Detection ELISA^{PLUS} kit. Likewise, the results (Fig. 2B) revealed that the formation of DNA fragments elicited by curcumin treatment was concentration-dependent in both ACC-2 and ACC-M cells, also more prominent in ACC-M cells ($P < 0.05$). Since curcumin is a tested inhibitor of NF-κB, which has been demonstrated to be more activated in ACC-M cells. And more importantly, we indeed found that

Downloaded from molpharm.aspetjournals.org at ASPET Journals on April 19, 2024

Molecular Pharmacology Fast Forward. Published on October 19, 2010 as DOI: 10.1124/mol.110.066910
This article has not been copyedited and formatted. The final version may differ from this version.

the capacity of curcumin in growth-inhibition and apoptosis-induction is likely more prominent in the high metastasis cell line ACC-M when compared with that in the low metastasis cell line ACC-2, suggesting high specificity. Thus, the ACC-M cell line was chosen for further apoptosis detection, as well as the subsequent migration/invasion, angiogenesis-induction, and mechanism studies.

Further confirmation of apoptosis-induction was determined by Annexin V-FITC and PI double-staining, which can quantitatively assess the early apoptotic and late apoptotic cell population. Of interest, the results showed that treatment with curcumin for 12 h concentration-dependently induced the early apoptosis of ACC-M cells, but the proportion of late-apoptotic cells was not significantly increased (Fig. 2C, *left*). This may well explain why exposure to curcumin for 12 h did not result in significant cell death, but only decreased the cell growth activity, as revealed by cell growth analysis and viability measurement (Fig. 1, B and D). However, after 24 h treatment with curcumin, both the early- and late-apoptotic cell population, especially the later one, were significantly increased (Fig. 2C, *right*), which confirmed the apoptosis-induction by curcumin. On the other hand, the activities of caspase-9 and caspase-3 were found to increase significantly in curcumin-treated ACC-M cells (Fig. 2D, *left*). Also the results showed that both the ratio of Bax/Bcl-2 and cleavage of PARP were significantly increased by curcumin in a concentration-dependent manner (Fig. 2D, *right*).

Curcumin Inhibits Migration and Invasion of ACC-M cells. The influence of curcumin on ACC cell migration and invasion was determined using the wound healing and Transwell Boyden chamber assays. As the results, both the migration and invasion of ACC-M cells were significantly impaired after curcumin treatment in a concentration-dependent manner (Fig. 3A). Meanwhile, the results also revealed that the mRNA expression and protein secretion of both MMP-2 and MMP-9 were down-regulated by curcumin treatment (Fig. 3D), which might explain the impaired migration and invasion ability of ACC-M cells.

Curcumin Inhibits ACC-Induced Angiogenesis *In Vitro* and *In Vivo*. It is clearly seen from the results (Fig. 3B) that the CM from ACC-M cells without curcumin pretreatment induced EAhy926 cell migration by four-fold compared to the control (blank medium). However, curcumin

Downloaded from molpharm.aspetjournals.org at ASPET Journals on April 19, 2024

Molecular Pharmacology Fast Forward. Published on October 19, 2010 as DOI: 10.1124/mol.110.066910
This article has not been copyedited and formatted. The final version may differ from this version.

pretreatment produced a concentration-dependent prevention of the endothelial cell migration induced by CM. Moreover, a similar result was also observed in the tube formation assay that curcumin concentration-dependently prevented the tube-like structure formation induced by ACC-M cells (Fig. 3B).

The rat aortic ring, CAM, as well as Matrigel plug assays were then performed to further confirm the inhibitory effects of curcumin on ACC-induced angiogenesis *in vivo*. As shown in Fig. 3C, treatment with curcumin resulted in a significant decrease in vessel sprouting at the cut edge of rat aortic rings. In addition, the CAM assay demonstrated that the newly formed vessels were markedly reduced when incubated with the CM from curcumin-treated ACC-M cells. Importantly, the Matrigel plug assay also showed similar results that the ability of ACC-M cells to induce angiogenesis was significantly impaired after curcumin pretreatment.

Additionally, the results also unmasked possible mechanisms that exposure of ACC-M cells to curcumin led to the suppression of VEGF and bFGF in both mRNA and protein levels (Fig. 3D), but showed no effect on G-CSF, PDGF or IL-6 production (data not shown).

Curcumin Dually Inhibits the mTOR and NF-κB Pathways Through a Crossed PI3K/Akt/IKK Signaling Axis. As the results show, curcumin significantly suppressed the activation of PI3K, Akt, IKKα, IKKβ, NF-κB, as well as mTOR and S6 in ACC cells in a concentration-dependent and time-dependent manner (Fig. 4A), but showed no effect on the phosphorylation status of ERK, p38, and JNK (data not shown). As shown in Fig. 4B, over-expression of CA-Akt nearly blocked curcumin-mediated IKKα inactivation, but only partially retrieved the down-regulation of NF-κB by curcumin. It also only partially prevented curcumin-induced apoptosis as revealed by the Cell Death Detection ELISA^{PLUS}. However, it showed no influence on curcumin-mediated IKKβ inactivation, indicating that the activity of IKKβ in ACC was probably Akt-independent.

Further investigation indeed validated this hypothesis in that LY294002, a specific PI3K inhibitor, effectively suppressed the phosphorylation of Akt and IKKα (Fig. 4C) in absence of curcumin, but there was no significant decrease in the phosphorylation level of IKKβ. In addition, LY294002 significantly eliminated the inhibitory effects of curcumin on Akt and IKKα, and meanwhile partially

Downloaded from molpharm.aspetjournals.org at ASPET Journals on April 19, 2024

Molecular Pharmacology Fast Forward. Published on October 19, 2010 as DOI: 10.1124/mol.110.066910
This article has not been copyedited and formatted. The final version may differ from this version.

blocked curcumin-induced cell apoptosis as well as mTOR and NF-κB down-regulation. Similarly, PS1145, a specific IKKα/β inhibitor, almost completely blocked the influence of curcumin on NF-κB activation, but only partially prevented the apoptosis-induction and mTOR-inhibition, manifested as following curcumin treatment could still induce further cell apoptosis as well as mTOR and S6 inactivation. Whereas, when LY294002 and PS1145 were used in combination, the responses of PI3K, Akt, IKKα, IKKβ, NF-κB, as well as mTOR and S6 to curcumin treatment were nearly abrogated (Fig. 4C), and the apoptosis-induction was also completed prevented. Collectively, these findings demonstrated that curcumin likely targets both the Akt-dependent IKKα and Akt-independent IKKβ, and finally leads to the dual-inhibition of both mTOR and NF-κB pathways. Nevertheless, the relationship between mTOR and NF-κB pathways is still unclear. Thus, the NF-κB inhibitor PDTC and mTOR inhibitor rapamycin, either alone or in combination, were then applied as shown in Fig. 4D. The results showed that treatment with PDTC alone effectively deleted the responses of NF-κB to curcumin, but only partially reversed the apoptosis induction by curcumin, and showed no effect on curcumin-mediated down-regulation of mTOR and S6. A similar insufficient effect was also revealed for rapamycin treatment alone. However, combined treatment with both PDTC and rapamycin almost abrogated all the effects of curcumin on NF-κB and mTOR pathways, as well as cell apoptosis, suggesting that the mTOR and NF-κB pathways are two major but independent downstream targets for curcumin-mediated inhibition in ACC. More vividly, the double-labeling immunofluorescence analyses revealed that the activity of mTOR and NF-κB were significantly and concurrently down-regulated by treatment with curcumin, accompanied by suppression of the Akt/IKK signaling axis (Supplementary Fig. 1). Thus, taken all the above results together, we may expect that curcumin may dually inhibit both mTOR and NF-κB pathways through a crossed PI3K/Akt/IKK signaling axis.

Curcumin Prevents Tumor Angiogenesis and Promotes Cell Apoptosis in ACC-M Xenografts. To further authenticate the striking anti-tumor effects of curcumin on ACC cells *in vitro*, xenografts in nude mice were used to verify the inhibitory activities of curcumin *in vivo*. As shown in Fig. 5, A and B, the growth of ACC-M tumors was obviously prevented by curcumin

Downloaded from molpharm.aspetjournals.org at ASPET Journals on April 19, 2024

Molecular Pharmacology Fast Forward. Published on October 19, 2010 as DOI: 10.1124/mol.110.066910
This article has not been copyedited and formatted. The final version may differ from this version.

treatment for 28 days, while no toxicity was observed. By performing the *in situ* TUNEL assay, we observed that there was a large increase in the number of apoptotic cells in the tumor tissues treated with curcumin (Fig. 5C). Moreover, the results also showed that the microvessels marked as CD31 positive staining were significantly reduced by curcumin treatment (Fig. 5C). To further correlate these *in vivo* tumor-therapeutic effects to the mechanisms identified *in vitro*, we then assessed the expression level of some key biomarkers in the tumor tissues by immunohistochemical analysis. As the results show, both VEGF and MMP-9 expressions were obviously down-regulated in curcumin-treated tumors concomitant with the suppression of NF-κB nuclear translocation and p-S6 activation (Fig. 5D). All the above results are consistent with the findings unmasked in our *in vitro* studies, and confirm that curucmin could effectively prevent tumor-induced angiogenesis and promote the apoptotic cell death of ACC by dual-inhibition of both mTOR and NF-κB pathways.

Concurrent High Activation Status of the mTOR and NF-κB Pathways in ACC. We next explored the nature activation status of both mTOR and NF-κB pathways in ACC tissues. Representative examples of immunohistochemical results of the selected cases are shown in Fig. 6A. Here, p-S6 was intensely stained in the cytoplasm of most ACC cells accompanied by a strong staining of p-mTOR in the cytoplasm and/or nuclei. Meanwhile, the nuclear staining of NF-κB was detected in some ACC cells at a mean rate of 14.3% in the same area. Moreover, the double-labeling immunofluorescence histochemistry analysis confirmed the concurrent activation of mTOR and NF-κB pathways in ACC (Fig. 6B). As shown in Supplementary Table, when the immunohistochemical staining of the tested markers in the ACC tissues was evaluated against NSG tissues, all of them were significantly higher in ACC cases across all the three histologic types. More importantly, the Spearman rank test revealed a significant correlation between the staining of p-mTOR and p-S6 (Supplementary Fig. 2A). Also both of them showed significant correlation with NF-κB activation (Supplementary Fig. 2, B and C). Taken together, the above data demonstrate that both mTOR and NF-κB pathways are ubiquitously activated in ACC and may concurrently play important roles in its malignant progression.

Downloaded from molpharm.aspetjournals.org at ASPET Journals on April 19, 2024

Molecular Pharmacology Fast Forward. Published on October 19, 2010 as DOI: 10.1124/mol.110.066910
This article has not been copyedited and formatted. The final version may differ from this version.

Additionally, the results also showed that the activation status of both mTOR and NF-κB pathways in the high metastasis cell line ACC-M were significantly higher than that in the low metastasis cell line ACC-2, correlating with the higher activation level of the PI3K/Akt/IKK signaling axis (Supplementary Fig. 3A). These findings in ACC cell cultures were consistent with those demonstrated in ACC tissue specimens, which further implicated the clinical significance of the concurrent activation of mTOR and NF-κB pathways in ACC progression. More importantly, a significant synergism in induction of apoptosis was observed in ACC-M cells after treatment with the combination of NF-κB and mTOR inhibitors compared with either NF-κB or mTOR inhibition alone (Supplementary Fig. 3B), demonstrating the strong rationale for dual-targeted therapies against this aggressive tumor.

Downloaded from molpharm.aspetjournals.org at ASPET Journals on April 19, 2024

Molecular Pharmacology Fast Forward. Published on October 19, 2010 as DOI: 10.1124/mol.110.066910
This article has not been copyedited and formatted. The final version may differ from this version.

Discussion

In the present study, we initially conducted *in vitro* studies and found that curcumin significantly inhibited the growth of ACC cells via the induction of apoptosis. Moreover, the migration/invasion and angiogenesis-induction of ACC cells was also attenuated by curcumin, and even earlier than the appearance of late apoptosis. We further applied a clinically relevant nude mouse xenograft model to evaluate the therapeutic effects of curcumin on ACC progression and found that curcumin treatment efficiently prevented the *in vivo* growth and angiogenesis of ACC tumors. These results suggest that further clinical investigation is warranted to apply curcumin as a novel therapeutic regimen for ACC.

Previous research has indicated that NF-κB is tightly involved in the malignant progression of ACC (Sun et al., 2010a; Zhang and Peng, 2007; Zhang and Peng, 2009; Zhang et al., 2005). Meanwhile, curcumin has been widely accepted as a potent inhibitor of NF-κB (Anand et al., 2008; Kunnumakkara et al., 2008; Kunnumakkara et al., 2007; Wang et al., 2008). Thus, it is reasonable for us to identify NF-κB as an eventual target of curcumin for the inhibitory activities in ACC as well. Our results indicated that curcumin significantly inhibited the nuclear translocation of NF-κB, accompanied by decreased IKK-α/β phosphorylation and up-regulated IκB-α expression, suggesting the involvement of IKK/NF-κB pathway in the inhibition of ACC by curcumin.

PI3K/Akt pathway-regulated NF-κB activation, through a p38/IKKβ-dependent or an IKKα-dependent mechanism (Viatour et al., 2005), plays essential roles in the malignant development of various tumors (Viatour et al., 2005; Zhang et al., 2007). Importantly, our previous study has indicated that the PI3K/Akt pathway was also intensively involved in the NF-κB activation in ACC (Sun et al., 2010a). Therefore, to investigate whether curcumin-mediated down-regulation of IKK/NF-κB interferes with the PI3K/Akt signaling axis, we examined the effect of curcumin on the PI3K/Akt pathway. Consequently, curcumin significantly suppressed the PI3K/Akt pathway, based on the observation of down-regulated phosphorylation levels of both PI3K and Akt. In contrast, curcumin had no effect on the MAPK signaling pathways, as represented by the unchanged phosphorylation status of ERK, p38, and JNK, which further

Downloaded from molpharm.aspetjournals.org at ASPET Journals on April 19, 2024

Molecular Pharmacology Fast Forward. Published on October 19, 2010 as DOI: 10.1124/mol.110.066910
This article has not been copyedited and formatted. The final version may differ from this version.

exclude the suppression of Akt/p38/IKKβ pathway from the possible mechanisms underlying curcumin-induced NF-κB down-regulation in ACC. Thus it might be hypothesized that the inhibitory activity of curcumin in ACC cells is probably due, at least in part, to its down-regulation of IKK/NF-κB pathway, both Akt-dependent and Akt-independent.

To validate our hypothesis and gain more insights into the mechanism by which curcumin inhibits ACC, we initially evaluate the influence of CA-Akt over-expression on curcumin-mediated inhibitory effects on ACC cells. As expected, transfection of ACC-M cells with CA-Akt efficiently reversed curcumin-induced inhibition of IKKα, but showed less effect on IKKβ inactivation, which might be responsible for the still obviously observed apoptosis-induction and NF-κB inactivation by curcumin. Furthermore, the results also showed that pretreatment with the IKK inhibitor PS1145 or NF-κB inhibitor PDTC could eliminate the effects of curcumin on NF-κB activation. However, we unexpectedly found that the apoptosis-induction by curcumin was only partially prevented by PS1145 or NF-κB pretreatment. These results suggest that the down-regulation of NF-κB may only partially contribute to the inhibitory effects of curcumin, and it is unlikely to be the sole component targeted by curcumin.

Considering the above observations, we turned to explore other possible components targeted by curcumin, especially those common downstream molecules of both Akt and IKKβ. Notably, mTOR, a highly conserved serine/threonine kinase, is one such molecular that has been shown to play critical roles in cancer initiation and progression (Guertin and Sabatini, 2007; Li et al., 2007) through Akt-, IKKβ-, and/or MAPK-dependent pathways (Lee et al., 2007). Additionally, despite unclear underlying mechanism, curcumin has been reported to inhibit mTOR activation in other cancer cells (Beevers et al., 2006; Li et al., 2007; Yu et al., 2008). So we tested the effect of curcumin on mTOR activation in ACC cells, and found that curcumin could potently decrease the phosphorylation level of mTOR as well as its downstream effector S6. To further determine the functional significance of the mTOR-suppression in curcumin-mediated inhibitory activities, ACC-M cells were pretreated with the specific inhibitor of mTOR, rapamycin, followed by exposure to curcumin. Similar to the effect of PDTC, rapamycin only partially reversed the cell apoptosis induced by curcumin, and showed no effect on curcumin-mediated NF-κB down-regulation, which

Downloaded from molpharm.aspetjournals.org at ASPET Journals on April 19, 2024

Molecular Pharmacology Fast Forward. Published on October 19, 2010 as DOI: 10.1124/mol.110.066910
This article has not been copyedited and formatted. The final version may differ from this version.

repeatedly suggested a concurrent suppression of both the NF-κB and mTOR pathways by curcumin. To make this conclusion more convincing, we pretreated ACC cells with both rapamycin and PDTC, followed by exposure to curcumin. As the result, combination of PDTC and rapamycin almost abrogated all the effects of curcumin on NF-κB and mTOR pathways, as well as cell apoptosis, confirming that the inhibitory activities of curcumin in ACC are highly dependent on its dual-suppression of both NF-κB and mTOR pathways. Furthermore, the results also revealed that curcumin-mediated dual-suppression of both NF-κB and mTOR pathways were both Akt- and IKKβ-dependent, as demonstrated by the significant difference for combination treatment compared with either PS1145 or LY294002 alone.

To make the above findings more clinically significant and therapeutically meaningful, we then explored the nature activation status of both the mTOR and NF-κB pathways in ACC. As shown in our previous study (Sun et al., 2010a), the NF-κB pathway was ubiquitously activated in ACC through the PI3K/Akt/IKK signaling axis. Here we further confirmed its concurrence with mTOR activation. Our results suggested that the mTOR and NF-κB pathways were indeed concurrently activated in ACC tissues. In an attempt to gain more insights into the concurrent activation of the mTOR and NF-κB pathways, two ACC cell lines were fully utilized. Previous studies, including those from our laboratory (Sun et al., 2010a; Zhang and Peng, 2007; Zhang and Peng, 2009; Zhang et al., 2005), have revealed that comparing with ACC-2 cells, ACC-M cells appeared more potent in invasive growth, apoptosis-evasion, angiogenesis-induction and distant metastasis. However, the precise molecular mechanisms underlying the malignant difference between these two cell lines are still far from clear. Here we unmasked for the first time that the activation status of both mTOR and NF-κB pathways in the high metastasis cell line ACC-M were significantly higher than that in the low metastasis cell line ACC-2, correlating with the higher activation level of the PI3K/Akt/IKK signaling axis. These findings were consistent with the results on ACC tissue specimens, implicating the clinical significance of the concurrent activation of mTOR and NF-κB pathways in ACC progression. More importantly, these findings demonstrated the strong rationale for dual-suppression of these two pathways, namely that inhibition of only one component may be insufficient for satisfying therapeutic benefit, because the other component could compensate.

Downloaded from molpharm.aspetjournals.org at ASPET Journals on April 19, 2024

Molecular Pharmacology Fast Forward. Published on October 19, 2010 as DOI: 10.1124/mol.110.066910
This article has not been copyedited and formatted. The final version may differ from this version.

Herein, we test this logic using combined NF-κB and mTOR inhibitors. As the results, significant synergism in induction of apoptosis was observed in ACC-M cells after treatment with the combination relative to either NF-κB or mTOR inhibition alone. To our best knowledge, this is the first time that the NF-κB and mTOR pathways were reported to be ubiquitously and concurrently activated in ACC, especially revealing its potential role in malignant progression. These findings may not only lead to a better understanding of the molecular pathogenesis of ACC, but also provide a basis for a rational approach to develop dual-targeted therapies against this aggressive tumor, just like curcumin-treatment.

In conclusion, the present study shows that curcumin, a natural polyphenol derived from the spice turmeric (*Curcuma longa*), not only significantly inhibits the *in vitro* growth, migration/invasion, and angiogenesis-induction in ACC cells, but also effectively prevents the *in vivo* growth and angiogenesis of ACC tumors in mice, relating with the dual-inhibition of both mTOR and NF-κB pathways through a crossed PI3K/Akt/IKK signaling axis (Fig. 7). Most importantly, we also reveal that the mTOR and NF-κB pathways were concurrently activated and correlated with the malignant progression in ACC. Our findings systematically dissected the effects of curcumin on a crossed PI3K/Akt/IKK signaling axis in ACC, determined the importance of dual-suppression of both mTOR and NF-κB for the inhibitory activity of curcumin, and shed new light on the mechanisms of anticancer activities of curcumin, as well as demonstrated strong rationale for dual-targeted therapies against ACC.

Acknowledgement

We thank Prof. Silvio J. Gutkind and Dr. Vyomesh Patel in Oral and Pharyngeal Cancer Branch, NIDCR for advice on experiment design and manuscript editing, Prof. Ashok B. Kulkarni, and Elias Utreras in Functional Genomics Section, LCDB, NIDCR for critical reading.

Downloaded from molpharm.aspetjournals.org at ASPET Journals on April 19, 2024

Molecular Pharmacology Fast Forward. Published on October 19, 2010 as DOI: 10.1124/mol.110.066910
This article has not been copyedited and formatted. The final version may differ from this version.

Authorship Contribution

Participated in research design: Sun, Chen, Zhang, Hu, Zhao

Conducted experiments: Sun, Chen, Zhang, Hu, Liu, Zhou, Zhu, Zhao

Performed data analysis: Sun, Chen, Zhang, Zhao

Wrote or contributed to the writing of the manuscript: Sun, Chen, Zhang, Zhao

Downloaded from molpharm.aspetjournals.org at ASPET Journals on April 19, 2024

Molecular Pharmacology Fast Forward. Published on October 19, 2010 as DOI: 10.1124/mol.110.066910
This article has not been copyedited and formatted. The final version may differ from this version.

References

Aggarwal BB, Shishodia S, Takada Y, Banerjee S, Newman RA, Bueso-Ramos CE and Price JE (2005) Curcumin suppresses the paclitaxel-induced nuclear factor-kappaB pathway in breast cancer cells and inhibits lung metastasis of human breast cancer in nude mice. *Clin Cancer Res* **11**:7490-7498.

Aggarwal S, Ichikawa H, Takada Y, Sandur SK, Shishodia S and Aggarwal BB (2006) Curcumin (diferuloylmethane) down-regulates expression of cell proliferation and antiapoptotic and metastatic gene products through suppression of IkappaBalpha kinase and Akt activation. *Mol Pharmacol* **69**:195-206.

Anand P, Sundaram C, Jhurani S, Kunnumakkara AB and Aggarwal BB (2008) Curcumin and cancer: an "old-age" disease with an "age-old" solution. *Cancer Lett* **267**:133-164.

Beevers CS, Li F, Liu L and Huang S (2006) Curcumin inhibits the mammalian target of rapamycin-mediated signaling pathways in cancer cells. *Int J Cancer* **119**:757-764.

Chen A and Zheng S (2008) Curcumin inhibits connective tissue growth factor gene expression in activated hepatic stellate cells in vitro by blocking NF-kappaB and ERK signalling. *Br J Pharmacol* **153**:557-567.

Dhillon N, Aggarwal BB, Newman RA, Wolff RA, Kunnumakkara AB, Abbruzzese JL, Ng CS, Badmaev V and Kurzrock R (2008) Phase II trial of curcumin in patients with advanced pancreatic cancer. *Clin Cancer Res* **14**:4491-4499.

Fordice J, Kershaw C, El-Naggar A and Goepfert H (1999) Adenoid cystic carcinoma of the head and neck: predictors of morbidity and mortality. *Arch Otolaryngol Head Neck Surg* **125**:149-152.

Goel A, Kunnumakkara AB and Aggarwal BB (2008) Curcumin as "Curecumin": from kitchen to clinic. *Biochem Pharmacol* **75**:787-809.

Guan XF, Qiu WL, He RG and Zhou XJ (1997) Selection of adenoid cystic carcinoma cell clone highly metastatic to the lung: an experimental study. *Int J Oral Maxillofac Surg* **26**:116-119.

Guertin DA and Sabatini DM (2007) Defining the role of mTOR in cancer. *Cancer Cell* **12**:9-22.

Hotte SJ, Winquist EW, Lamont E, MacKenzie M, Vokes E, Chen EX, Brown S, Pond GR, Murgo A and Siu LL (2005) Imatinib mesylate in patients with adenoid cystic cancers of the salivary glands expressing c-kit: a Princess Margaret Hospital phase II consortium study. *J Clin Oncol*

Downloaded from molpharm.aspetjournals.org at ASPET Journals on April 19, 2024

Molecular Pharmacology Fast Forward. Published on October 19, 2010 as DOI: 10.1124/mol.110.066910
This article has not been copyedited and formatted. The final version may differ from this version.

23:585-590.

Kunnumakkara AB, Diagaradjane P, Guha S, Deorukhkar A, Shentu S, Aggarwal BB and Krishnan S (2008) Curcumin sensitizes human colorectal cancer xenografts in nude mice to gamma-radiation by targeting nuclear factor-kappaB-regulated gene products. *Clin Cancer Res* **14**:2128-2136.

Kunnumakkara AB, Guha S, Krishnan S, Diagaradjane P, Gelovani J and Aggarwal BB (2007) Curcumin potentiates antitumor activity of gemcitabine in an orthotopic model of pancreatic cancer through suppression of proliferation, angiogenesis, and inhibition of nuclear factor-kappaB-regulated gene products. *Cancer Res* **67**:3853-3861.

Lao CD, Ruffin MTt, Normolle D, Heath DD, Murray SI, Bailey JM, Boggs ME, Crowell J, Rock CL and Brenner DE (2006) Dose escalation of a curcuminoid formulation. *BMC Complement Altern Med* **6**:10.

Lee DF, Kuo HP, Chen CT, Hsu JM, Chou CK, Wei Y, Sun HL, Li LY, Ping B, Huang WC, He X, Hung JY, Lai CC, Ding Q, Su JL, Yang JY, Sahin AA, Hortobagyi GN, Tsai FJ, Tsai CH and Hung MC (2007) IKK beta suppression of TSC1 links inflammation and tumor angiogenesis via the mTOR pathway. *Cell* **130**:440-455.

Lee DF, Kuo HP, Chen CT, Wei Y, Chou CK, Hung JY, Yen CJ and Hung MC (2008) IKKbeta suppression of TSC1 function links the mTOR pathway with insulin resistance. *Int J Mol Med* **22**:633-638.

Lev-Ari S, Starr A, Vexler A, Karaush V, Loew V, Greif J, Fenig E, Aderka D and Ben-Yosef R (2006) Inhibition of pancreatic and lung adenocarcinoma cell survival by curcumin is associated with increased apoptosis, down-regulation of COX-2 and EGFR and inhibition of Erk1/2 activity. *Anticancer Res* **26**:4423-4430.

Li L, Aggarwal BB, Shishodia S, Abbruzzese J and Kurzrock R (2004) Nuclear factor-kappaB and IkappaB kinase are constitutively active in human pancreatic cells, and their down-regulation by curcumin (diferuloylmethane) is associated with the suppression of proliferation and the induction of apoptosis. *Cancer* **101**:2351-2362.

Li M, Zhang Z, Hill DL, Wang H and Zhang R (2007) Curcumin, a dietary component, has anticancer, chemosensitization, and radiosensitization effects by down-regulating the MDM2 oncogene through the PI3K/mTOR/ETS2 pathway. *Cancer Res* **67**:1988-1996.

Downloaded from molpharm.aspetjournals.org at ASPET Journals on April 19, 2024

Molecular Pharmacology Fast Forward. Published on October 19, 2010 as DOI: 10.1124/mol.110.066910
This article has not been copyedited and formatted. The final version may differ from this version.

Lin YG, Kunnumakkara AB, Nair A, Merritt WM, Han LY, Armaiz-Pena GN, Kamat AA, Spannuth WA, Gershenson DM, Lutgendorf SK, Aggarwal BB and Sood AK (2007) Curcumin inhibits tumor growth and angiogenesis in ovarian carcinoma by targeting the nuclear factor-kappaB pathway. *Clin Cancer Res* **13**:3423-3430.

Milacic V, Banerjee S, Landis-Piwowar KR, Sarkar FH, Majumdar AP and Dou QP (2008) Curcumin inhibits the proteasome activity in human colon cancer cells in vitro and in vivo. *Cancer Res* **68**:7283-7292.

Padhye S, Chavan D, Pandey S, Deshpande J, Swamy KV and Sarkar FH (2010) Perspectives on Chemopreventive and Therapeutic Potential of Curcumin Analogs in Medicinal Chemistry. *Mini Rev Med Chem*.

Persson M, Andren Y, Mark J, Horlings HM, Persson F and Stenman G (2009) Recurrent fusion of MYB and NFIB transcription factor genes in carcinomas of the breast and head and neck. *Proc Natl Acad Sci U S A* **106**:18740-18744.

Seeliger H, Guba M, Kleespies A, Jauch KW and Bruns CJ (2007) Role of mTOR in solid tumor systems: a therapeutical target against primary tumor growth, metastases, and angiogenesis. *Cancer Metastasis Rev* **26**:611-621.

Shankar S, Ganapathy S, Chen Q and Srivastava RK (2008) Curcumin sensitizes TRAIL-resistant xenografts: molecular mechanisms of apoptosis, metastasis and angiogenesis. *Mol Cancer* **7**:16.

Shishodia S, Amin HM, Lai R and Aggarwal BB (2005) Curcumin (diferuloylmethane) inhibits constitutive NF-kappaB activation, induces G1/S arrest, suppresses proliferation, and induces apoptosis in mantle cell lymphoma. *Biochem Pharmacol* **70**:700-713.

Sun ZJ, Chen G, Hu X, Zhang W, Liu Y, Zhu LX, Zhou Q and Zhao YF (2010a) Activation of PI3K/Akt/IKK-alpha/NF-kappaB signaling pathway is required for the apoptosis-evasion in human salivary adenoid cystic carcinoma: its inhibition by quercetin. *Apoptosis* **15**:850-863.

Sun ZJ, Chen G, Zhang W, Hu X, Huang CF, Wang YF, Jia J and Zhao YF (2010b) Mammalian Target of Rapamycin Pathway Promotes Tumor-Induced Angiogenesis in Adenoid Cystic Carcinoma: Its Suppression by Isoliquiritigenin through Dual Activation of c-Jun NH2-Terminal Kinase and Inhibition of Extracellular Signal-Regulated Kinase. *J Pharmacol Exp Ther* **334**:500-512.

Downloaded from molpharm.aspetjournals.org at ASPET Journals on April 19, 2024

Molecular Pharmacology Fast Forward. Published on October 19, 2010 as DOI: 10.1124/mol.110.066910
This article has not been copyedited and formatted. The final version may differ from this version.

Viatour P, Merville MP, Bours V and Chariot A (2005) Phosphorylation of NF-kappaB and IkappaB proteins: implications in cancer and inflammation. *Trends Biochem Sci* **30**:43-52.

Wang D, Veena MS, Stevenson K, Tang C, Ho B, Suh JD, Duarte VM, Faull KF, Mehta K, Srivatsan ES and Wang MB (2008) Liposome-encapsulated curcumin suppresses growth of head and neck squamous cell carcinoma in vitro and in xenografts through the inhibition of nuclear factor kappaB by an AKT-independent pathway. *Clin Cancer Res* **14**:6228-6236.

Yodkeeree S, Chaiwangyen W, Garbisa S and Limtrakul P (2008) Curcumin, demethoxycurcumin and bisdemethoxycurcumin differentially inhibit cancer cell invasion through the down-regulation of MMPs and uPA. *J Nutr Biochem*.

Yoysungnoen P, Wirachwong P, Bhattarakosol P, Niimi H and Patumraj S (2006) Effects of curcumin on tumor angiogenesis and biomarkers, COX-2 and VEGF, in hepatocellular carcinoma cell-implanted nude mice. *Clin Hemorheol Microcirc* **34**:109-115.

Yu S, Shen G, Khor TO, Kim JH and Kong AN (2008) Curcumin inhibits Akt/mammalian target of rapamycin signaling through protein phosphatase-dependent mechanism. *Mol Cancer Ther* **7**:2609-2620.

Zhang J and Peng B (2007) In vitro angiogenesis and expression of nuclear factor kappaB and VEGF in high and low metastasis cell lines of salivary gland Adenoid Cystic Carcinoma. *BMC Cancer* **7**:95.

Zhang J and Peng B (2009) NF-kappaB promotes iNOS and VEGF expression in salivary gland adenoid cystic carcinoma cells and enhances endothelial cell motility in vitro. *Cell Prolif* **42**:150-161.

Zhang J, Peng B and Chen X (2005) Expressions of nuclear factor kappaB, inducible nitric oxide synthase, and vascular endothelial growth factor in adenoid cystic carcinoma of salivary glands: correlations with the angiogenesis and clinical outcome. *Clin Cancer Res* **11**:7334-7343.

Zhang X, Jin B and Huang C (2007) The PI3K/Akt pathway and its downstream transcriptional factors as targets for chemoprevention. *Curr Cancer Drug Targets* **7**:305-316.

Downloaded from molpharm.aspetjournals.org at ASPET Journals on April 19, 2024

Molecular Pharmacology Fast Forward. Published on October 19, 2010 as DOI: 10.1124/mol.110.066910
This article has not been copyedited and formatted. The final version may differ from this version.

Footnotes

This study was supported in part by the National Natural Science Foundation of China [Grants 30872894 and 30973330]; and the National Undergraduate Innovative Experiment Project [Grant 091048654].

Zhi-Jun Sun and Gang Chen contributed equally to this work, and should be considered co-first authors.

The abstract of this article has been presented, and won the outstanding poster presentation Award in 19th International Conference of Oral and Maxillofacial Surgery.

Downloaded from molpharm.aspetjournals.org at ASPET Journals on April 19, 2024

Molecular Pharmacology Fast Forward. Published on October 19, 2010 as DOI: 10.1124/mol.110.066910
This article has not been copyedited and formatted. The final version may differ from this version.

Legends for figures

Fig. 1. Inhibitory effects of curcumin on ACC cell growth and viability. A and B, cell growth was measured by the CTG luminescent assay in 96-well plates in the presence of increasing concentrations of curcumin, as indicated, for 12, 24, 48, and 72 h, and the results were expressed as percent growth relative to 100% at the time of curcumin addition. C and D, cell viability was measured using the Vi-CELL cell viability analyzer. Treatment conditions were identical as indicated in the CTG assay, and results were represented as a percentage of the control group. All data are presented as mean from three different experiments with duplicate (*, $P < 0.05$; **, $P < 0.01$ versus the control group); bars, ±SE.

Fig. 2. Curcumin induces apoptosis in ACC cells. A, detection of apoptosis in ACC cells by Hoechst 33258 staining. ACC-M and ACC-2 cells were cultured with DMSO (Control) or curcumin (20 μM) for 24 h. Cells were then fixed and stained with a DNA specific dye, Hoechst 33258. B, quantitation of DNA fragmentation using the Cell Death Detection ELISA^{PLUS}. ACC-M and ACC-2 cells were treated with DMSO (Control) or indicated concentrations of curcumin for 24 h, and then analyzed using the Cell Death Detection ELISA^{PLUS} kit. C, representative dot plots of PI versus Annexin V-FITC. ACC-M cells were treated with DMSO (Control) or indicated concentrations of curcumin, and analyzed after 12 and 24 h, respectively. The lower left quadrant contains the vital (Annexin V^-/PI^-) population; the lower right contains the early apoptotic (Annexin V^+/PI^-) population; the upper right contains the late apoptotic (Annexin V^+/PI^+) population; and the upper left contains the necrotic (Annexin V^-/PI^+) population. Quantitative analysis showing the percentage of early and late apoptotic cells (*bottom*). D, the activities of caspase-9 and caspase-3 were assessed by Caspase Activity Assay kit (*left*). *Right*, the expression levels of cleaved PARP, Bax, and Bcl-2 were determined by Western blotting. Columns, mean; bars, ±SE. *, $P < 0.05$; **, $P < 0.01$ versus the control group.

Downloaded from molpharm.aspetjournals.org at ASPET Journals on April 19, 2024

Molecular Pharmacology Fast Forward. Published on October 19, 2010 as DOI: 10.1124/mol.110.066910
This article has not been copyedited and formatted. The final version may differ from this version.

Fig. 3. Curcumin inhibits the ability of ACC cells to migrate/invade as well as to induce angiogenesis i*n vitro* and *in vivo*. For cell migration/invasion detection, ACC-M cells were treated with or without indicated concentrations of curcumin for 12 h. For angiogenesis assays, ACC cells were further incubated with fresh serum-deprived medium in the absence of curcumin for another 24 h, followed by the collection of CM. A, inhibitory effects of curcumin on ACC cell migration and invasion were determined by the wound-healing migration assay, as well as the Transwell Boyden chamber with polycarbonate filters (8 μm pore size) coated without or with Matrigel, respectively. Migrated or invaded cells were counted and analyzed following a 12-h exposure to DMSO (Control) or indicated concentrations of curcumin. Columns, mean from three independent experiments; bars, ±SE. *, $P < 0.05$; **, $P < 0.01$ versus the control group. B and C, CM-induced *in vitro* migration and capillary network formation of EAhy926 cells (B), as well as CM-induced *in vivo* angiogenesis in the rat aortic ring, CAM and mouse Matrigel plug assays (C). Control panel indicates that a blank medium was added, while in the other two panels CM without or with curcumin pretreatment was added, as indicated. Percent inhibition was expressed using blank group as 100% (*bottom*). Columns, mean from three independent experiments; bars, ±SE. *, $P < 0.05$; **, $P < 0.01$ versus the CM without curcumin treatment group. D, the mRNA expression (*top*) and protein secretion (*bottom*) levels of VEGF, bFGF, MMP-2, and MMP-9 by ACC-M cells were determined by RT-PCR and ELISA, respectively, after a 12-h exposure to DMSO (Control) or indicated concentrations of curcumin. All data are presented as mean from three different experiments with duplicate (*, $P < 0.05$; **, $P < 0.01$ versus the control group); bars, ±SE.

Fig. 4. Curcumin dually inhibits the mTOR and NF-κB pathways through a crossed PI3K/Akt/IKK signaling axis. A, ACC-M cells were treated with indicated concentrations of curcumin in serum-deprived medium for indicated time. The expression levels of PI3K, Akt, IKKα/β, mTOR, S6 and their phosplorylation forms, as well as IκBα and nuclear form of NF-κB were determined by Western blotting. B, ACC-M cells were transfected with CA-Akt and vector plasmids, followed by incubation with curcumin (40 μM) in serum-deprived medium for 24 h. The expression levels of p-Akt, p-IKK and nuclear NF-κB were detected by Western blotting. C, ACC-M cells were

Downloaded from molpharm.aspetjournals.org at ASPET Journals on April 19, 2024

Molecular Pharmacology Fast Forward. Published on October 19, 2010 as DOI: 10.1124/mol.110.066910
This article has not been copyedited and formatted. The final version may differ from this version.

pretreated with LY294002 (20 μM) or/and PS1145 (10 μM) for 1 h, followed by incubation with curcumin (40 μM) in serum-deprived medium for 24 h. The expression levels of phosphor-form of mTOR, S6, IKK and Akt, as well as nuclear form of NF-κB were analyzed by Western blotting. D, ACC-M cells were pretreated with PDTC (20 μM) or/and rapamycin (100 nM) for 1 h, followed by incubation with with curcumin (40 μM) in serum-deprived medium for 24 h. The expression levels of p-mTOR, p-S6, p-IKK and p-Akt, as well as nuclear NF-κB were measured by Western blotting. Densitometric quantitation relative to the control is shown on the top of the immunoreactive bands. Cell apoptosis was assessed by quantitation of DNA fragmentation using Cell Death Detection ELISA^{PLUS} kit. Percent DNA fragmentation was calculated by considering 100% fragmentation unitedly at the time of curcumin addition. All data are presented as mean from three different experiments with duplicate (*, $P < 0.01$ versus DMSO-treated control cells, and †, $P < 0.01$ versus curcumin-treated cells without any other pretreatment); bars, ±SE.

Fig. 5. Curcumin prevents tumor growth *in vivo*. A, tumor regression observed in ACC xenografts treated with curcumin. ACC-M cells were used to establish xenografts in athymic nu/nu mice, and tumor-bearing animals were given with curcumin (1 g/kg, p.o., daily; n=8) or corn oil (Vehicle, 100 μL, p.o., daily; n=8) for 4 consecutive weeks. An example of tumor regression in curcumin-treated animals is depicted (*left*). *Right*, tumor size from ACC-M xenografts (*top*) and body weight of mice (*bottom*) in both vehicle- and curcumin-treated groups was assessed daily, as indicated. Points, mean; bars, ±SE. B, lesions dissected from ACC-M xenografts after treatment with vehicle or curcumin for 28 days. ANOVA followed by the Student-Newman-Keul's test was used to determine the difference between the curcumin- and vehicle-treated groups ($P < 0.001$) at day 28. C, Apoptotic cells as well as microvessels in both curcumin- and vehicle-treated ACC-M tumor tissues were determined by the *in situ* TUNEL assay as well as CD31 immunofluorescence staining, respectively. D, immunohistochemical analyses of the indicated biomarkers in both curcumin- and vehicle-treated ACC-M tumor tissues.

Downloaded from molpharm.aspetjournals.org at ASPET Journals on April 19, 2024

Molecular Pharmacology Fast Forward. Published on October 19, 2010 as DOI: 10.1124/mol.110.066910
This article has not been copyedited and formatted. The final version may differ from this version.

Fig. 6. Concurrent activation of mTOR and NF-κB pathways in ACC tissues. A, immunohistochemical staining of p-mTOR, p-S6, and NF-κB in both NSG and ACC tissues. B, double-labeling immunofluorescence histochemistry for p-S6 and NF-κB in both NSG and ACC tissues. The arrows indicate the concurrence of S6 activation and NF-κB nuclear translocation.

Fig. 7. Schematic representation of the proposed mechanisms underlying curcumin-mediated inhibitory effects on ACC progression. Curcumin specifically targets the PI3K/Akt/IKK signaling axis, which consequently leads to the concurrent but independent suppression of both NF-κB and mTOR pathways and concomitant activation of caspases as well as down-regulation of VEGF and MMPs, resulting in apoptosis-induction, angiogenesis-prevention as well as invasion-suppression, and finally causes the inhibition of ACC progression.

Downloaded from molpharm.aspetjournals.org at ASPET Journals on April 19, 2024

Figure 1

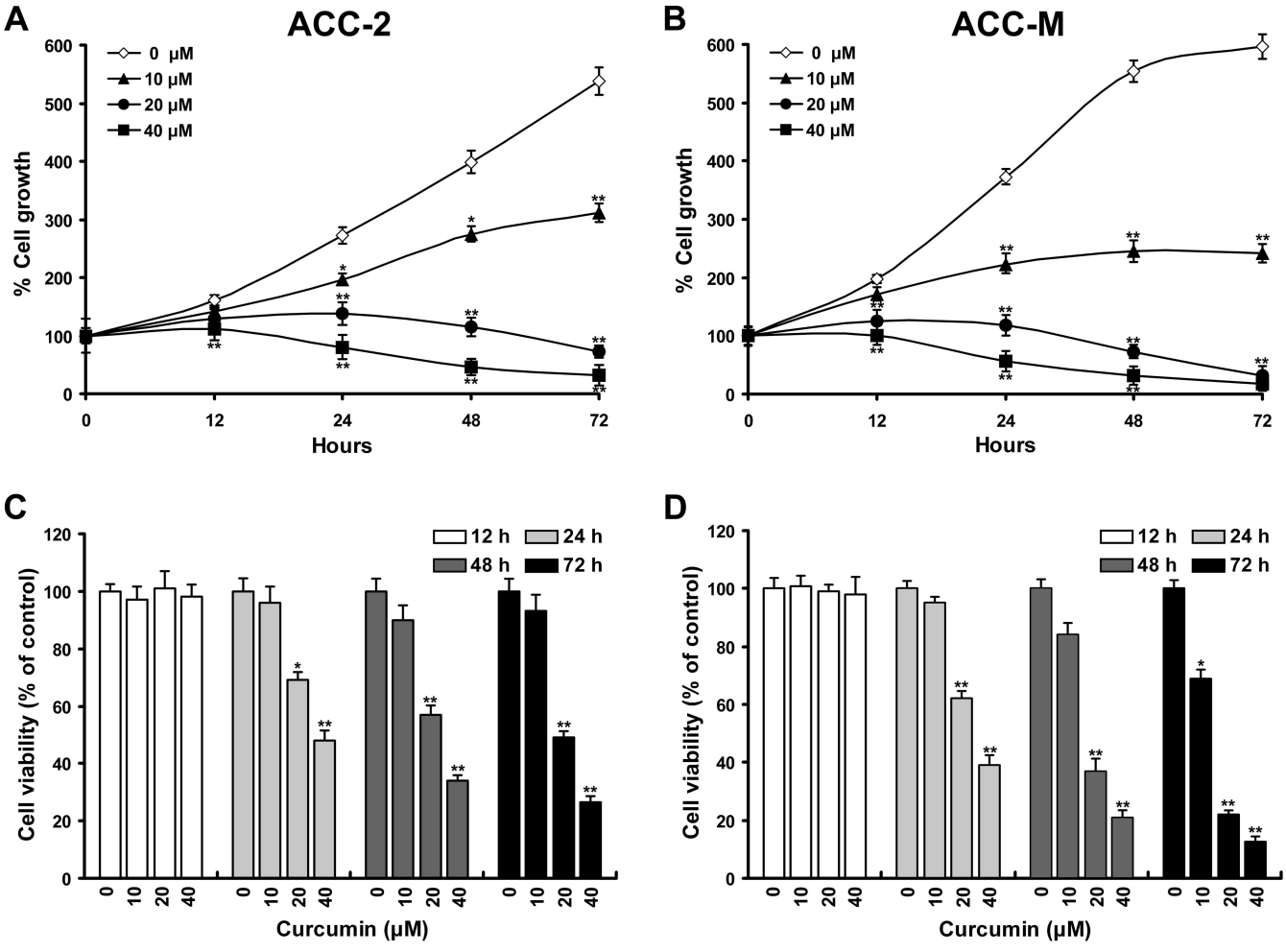
A
ACC-2
0 μM
10 μM
20 μM
40 μM
% Cell growth
Hours
B
ACC-M
C
12 h
24 h
48 h
72 h
Cell viability (% of control)
Curcumin (μM)
D

Figure 2

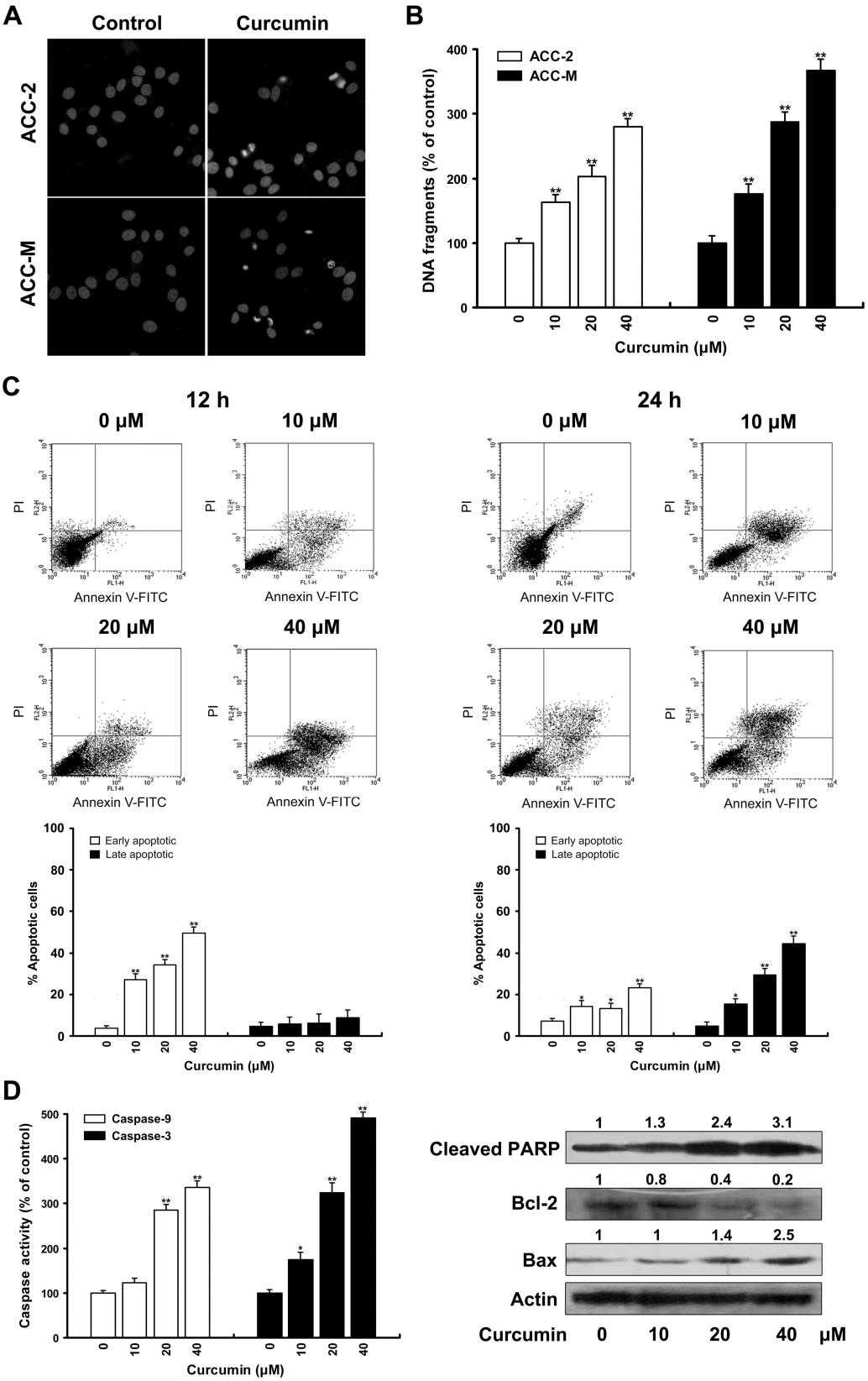
A
Control
Curcumin
ACC-2
ACC-M
B
ACC-2
ACC-M
DNA fragments (% of control)
Curcumin (μM)
C
12 h
24 h
0 μM
10 μM
20 μM
40 μM
PI
Annexin V-FITC
Early apoptotic
Late apoptotic
% Apoptotic cells
Curcumin (μM)
D
Caspase-9
Caspase-3
Caspase activity (% of control)
Curcumin (μM)
Cleaved PARP
Bcl-2
Bax
Actin
Curcumin
μM

Figure 3

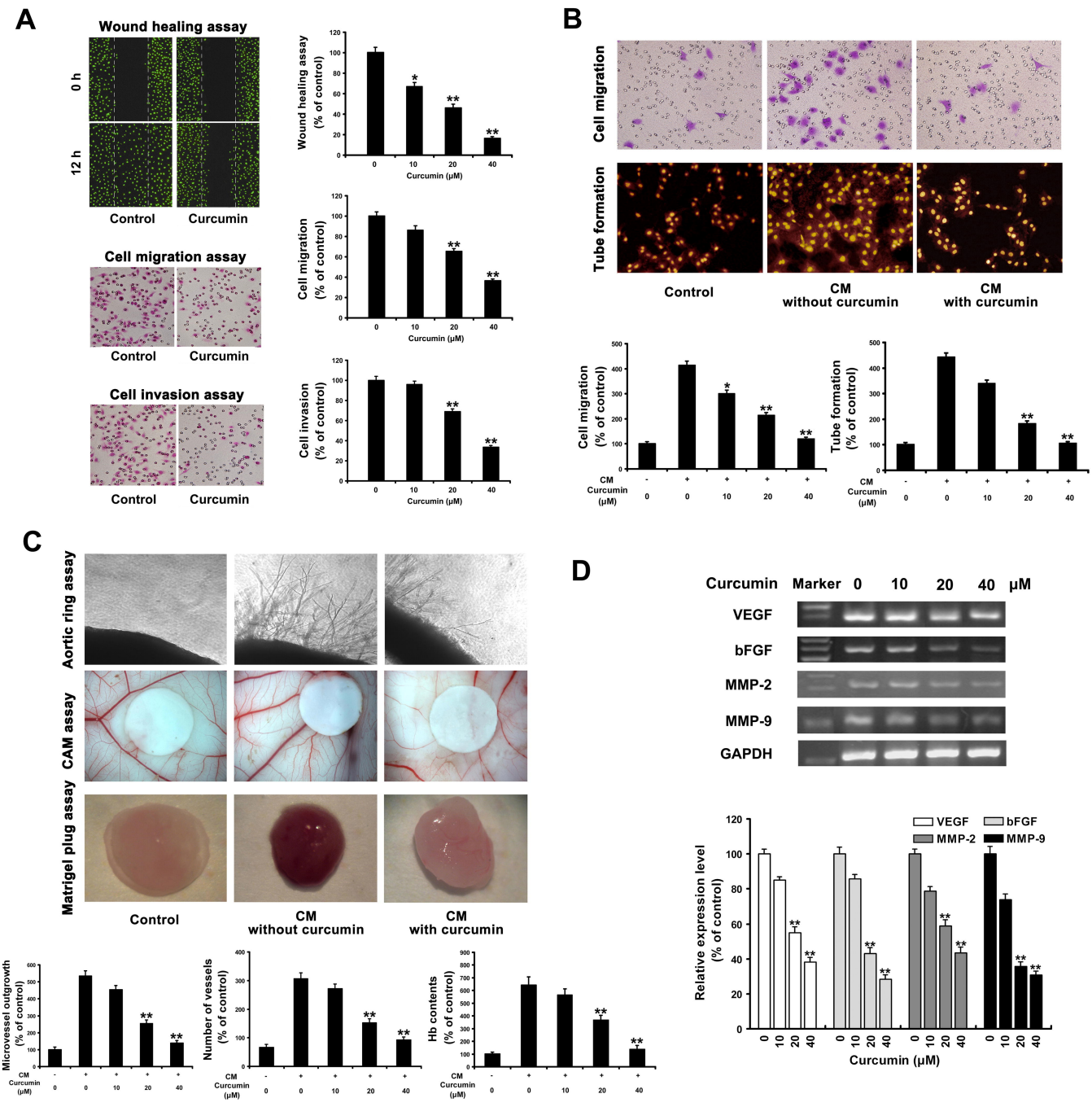
A
Wound healing assay
0 h
12 h
Control
Curcumin
Wound healing assay (% of control)
Curcumin (μM)
Cell migration assay
Cell migration (% of control)
Cell invasion assay
Cell invasion (% of control)
B
Cell migration
Tube formation
Control
CM without curcumin
CM with curcumin
CM
Curcumin (μM)
Tube formation (% of control)
C
Aortic ring assay
CAM assay
Matrigel plug assay
Microvessel outgrowth (% of control)
Number of vessels (% of control)
Hb contents (% of control)
D
Curcumin
Marker
μM
VEGF
bFGF
MMP-2
MMP-9
GAPDH
Relative expression level (% of control)
Curcumin (μM)

Figure 4

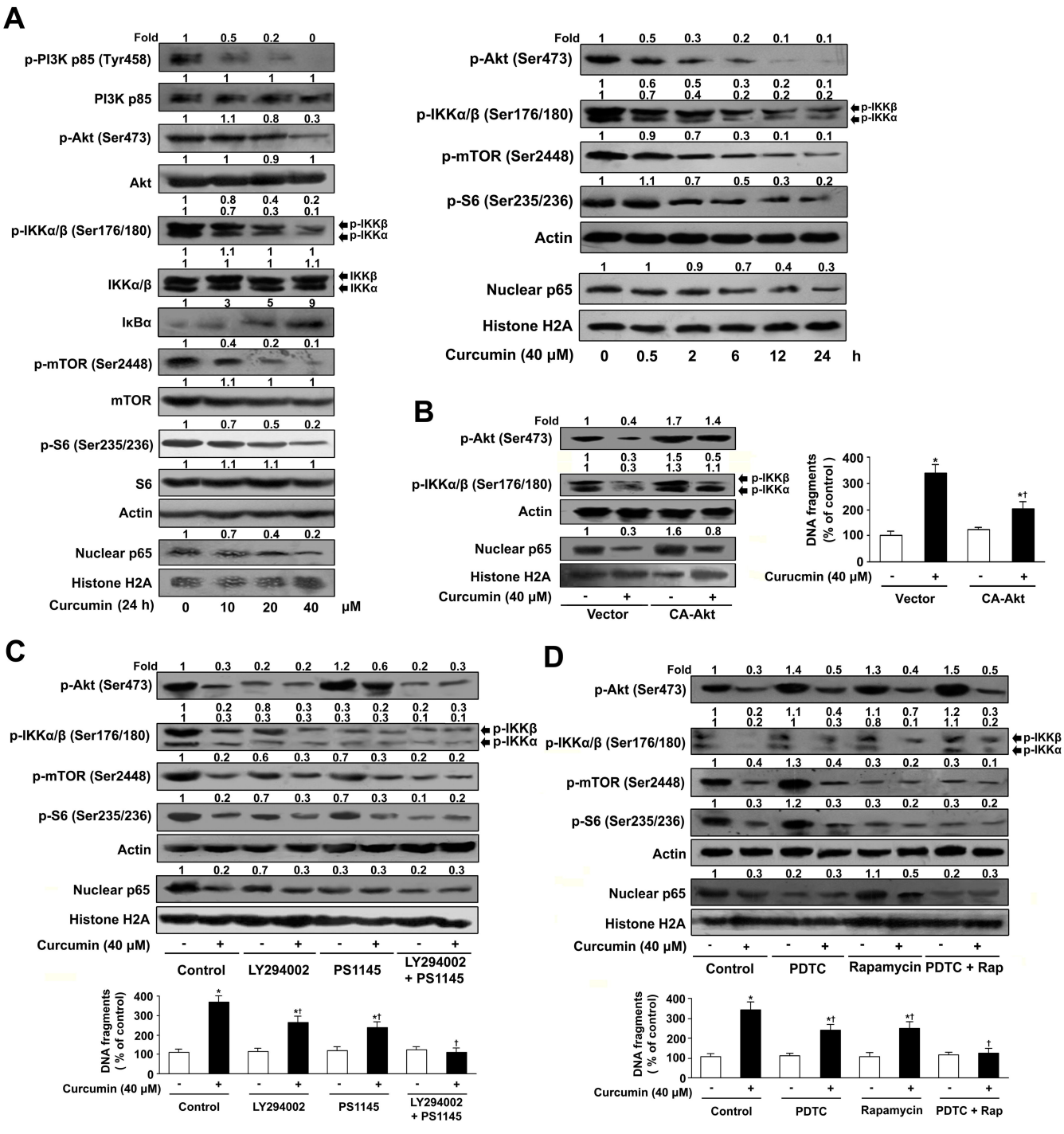
A
Fold 1 0.5 0.2 0
p-PI3K p85 (Tyr458)
1 1 1 1
PI3K p85
1 1.1 0.8 0.3
p-Akt (Ser473)
1 1 0.9 1
Akt
1 0.8 0.4 0.2
1 0.7 0.3 0.1
p-IKKα/β (Ser176/180)
p-IKKβ
p-IKKα
1 1.1 1 1
1 1 1 1.1
IKKα/β
IKKβ
IKKα
1 3 5 9
IκBα
1 0.4 0.2 0.1
p-mTOR (Ser2448)
1 1.1 1 1
mTOR
1 0.7 0.5 0.2
p-S6 (Ser235/236)
1 1.1 1.1 1
S6
Actin
1 0.7 0.4 0.2
Nuclear p65
Histone H2A
Curcumin (24 h) 0 10 20 40 μM
Fold 1 0.5 0.3 0.2 0.1 0.1
p-Akt (Ser473)
1 0.6 0.5 0.3 0.2 0.1
1 0.7 0.4 0.2 0.2 0.2
p-IKKα/β (Ser176/180)
p-IKKβ
p-IKKα
1 0.9 0.7 0.3 0.1 0.1
p-mTOR (Ser2448)
1 1.1 0.7 0.5 0.3 0.2
p-S6 (Ser235/236)
Actin
1 1 0.9 0.7 0.4 0.3
Nuclear p65
Histone H2A
Curcumin (40 μM) 0 0.5 2 6 12 24 h
B
Fold 1 0.4 1.7 1.4
p-Akt (Ser473)
1 0.3 1.5 0.5
1 0.3 1.3 1.1
p-IKKα/β (Ser176/180)
p-IKKβ
p-IKKα
Actin
1 0.3 1.6 0.8
Nuclear p65
Histone H2A
Curcumin (40 μM) - + - +
Vector CA-Akt
DNA fragments (% of control)
400
300
200
100
0
*
*†
Curucmin (40 μM) - + - +
Vector CA-Akt
C
Fold 1 0.3 0.2 0.2 1.2 0.6 0.2 0.3
p-Akt (Ser473)
1 0.2 0.8 0.3 0.3 0.2 0.2 0.3
1 0.3 0.3 0.3 0.3 0.3 0.1 0.1
p-IKKα/β (Ser176/180)
p-IKKβ
p-IKKα
1 0.2 0.6 0.3 0.7 0.3 0.2 0.2
p-mTOR (Ser2448)
1 0.2 0.7 0.3 0.7 0.3 0.1 0.2
p-S6 (Ser235/236)
Actin
1 0.2 0.7 0.3 0.3 0.3 0.2 0.3
Nuclear p65
Histone H2A
Curcumin (40 μM) - + - + - + - +
Control LY294002 PS1145 LY294002 + PS1145
DNA fragments (% of control)
400
300
200
100
0
*
*†
†
Curcumin (40 μM) - + - + - + - +
Control LY294002 PS1145 LY294002 + PS1145
D
Fold 1 0.3 1.4 0.5 1.3 0.4 1.5 0.5
p-Akt (Ser473)
1 0.2 1.1 0.4 1.1 0.7 1.2 0.3
1 0.2 1 0.3 0.8 0.1 1.1 0.2
p-IKKα/β (Ser176/180)
p-IKKβ
p-IKKα
1 0.4 1.3 0.4 0.3 0.2 0.3 0.1
p-mTOR (Ser2448)
1 0.3 1.2 0.3 0.3 0.2 0.3 0.2
p-S6 (Ser235/236)
Actin
1 0.3 0.2 0.3 1.1 0.5 0.2 0.3
Nuclear p65
Histone H2A
Curcumin (40 μM) - + - + - + - +
Control PDTC Rapamycin PDTC + Rap
DNA fragments (% of control)
400
300
200
100
0
*
*†
*†
†
Curcumin (40 μM) - + - + - + - +
Control PDTC Rapamycin PDTC + Rap

Figure 5

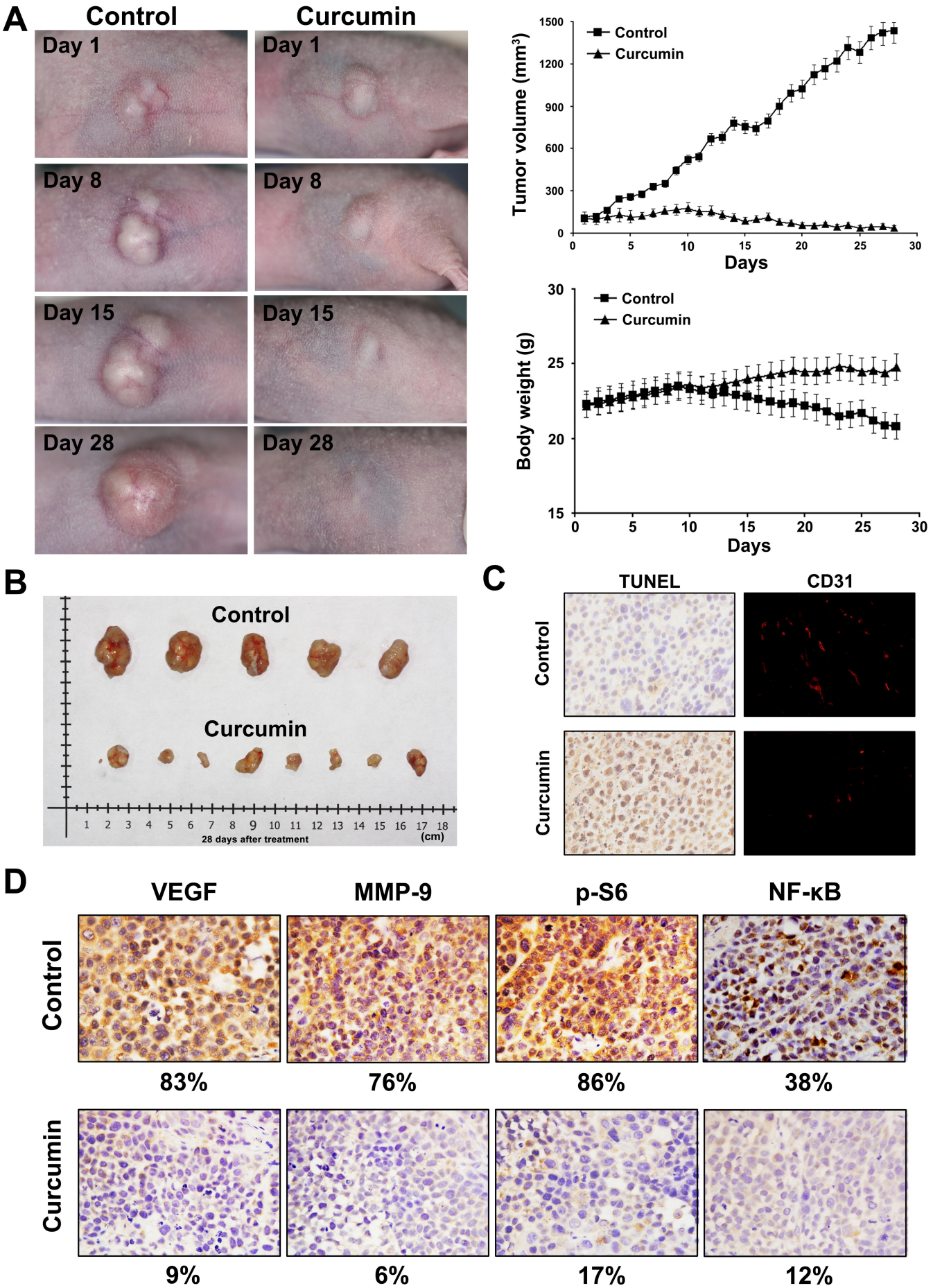
A
Control
Curcumin
Day 1
Day 1
Day 8
Day 8
Day 15
Day 15
Day 28
Day 28
Tumor volume (mm3)
Control
Curcumin
Days
Body weight (g)
Control
Curcumin
Days
B
Control
Curcumin
28 days after treatment
(cm)
C
TUNEL
CD31
Control
Curcumin
D
VEGF
MMP-9
p-S6
NF-κB
Control
83%
76%
86%
38%
Curcumin
9%
6%
17%
12%

Figure 6

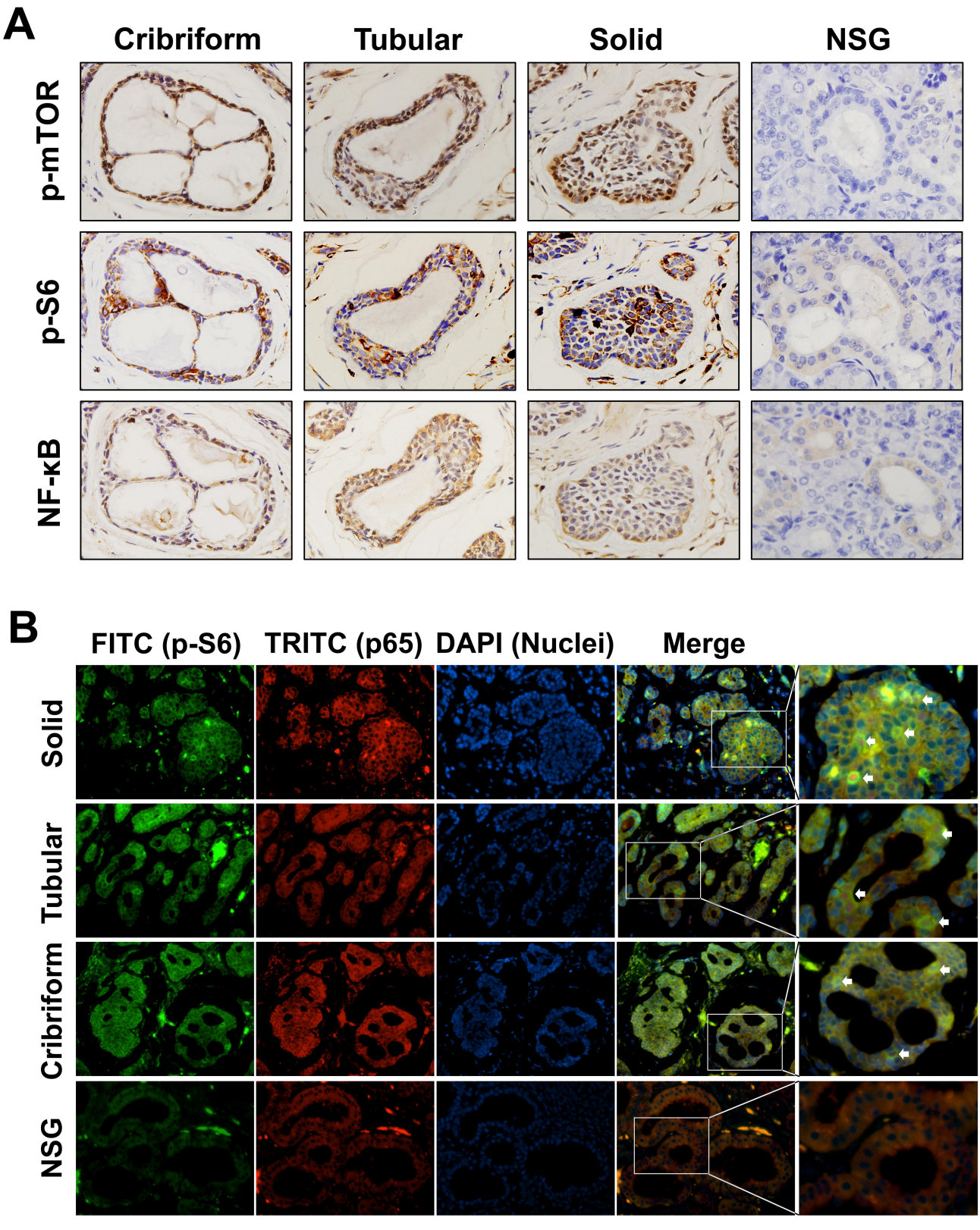
A
Cribriform
Tubular
Solid
NSG
p-mTOR
p-S6
NF-κB
B
FITC (p-S6)
TRITC (p65)
DAPI (Nuclei)
Merge
Solid
Tubular
Cribriform
NSG

Figure 7

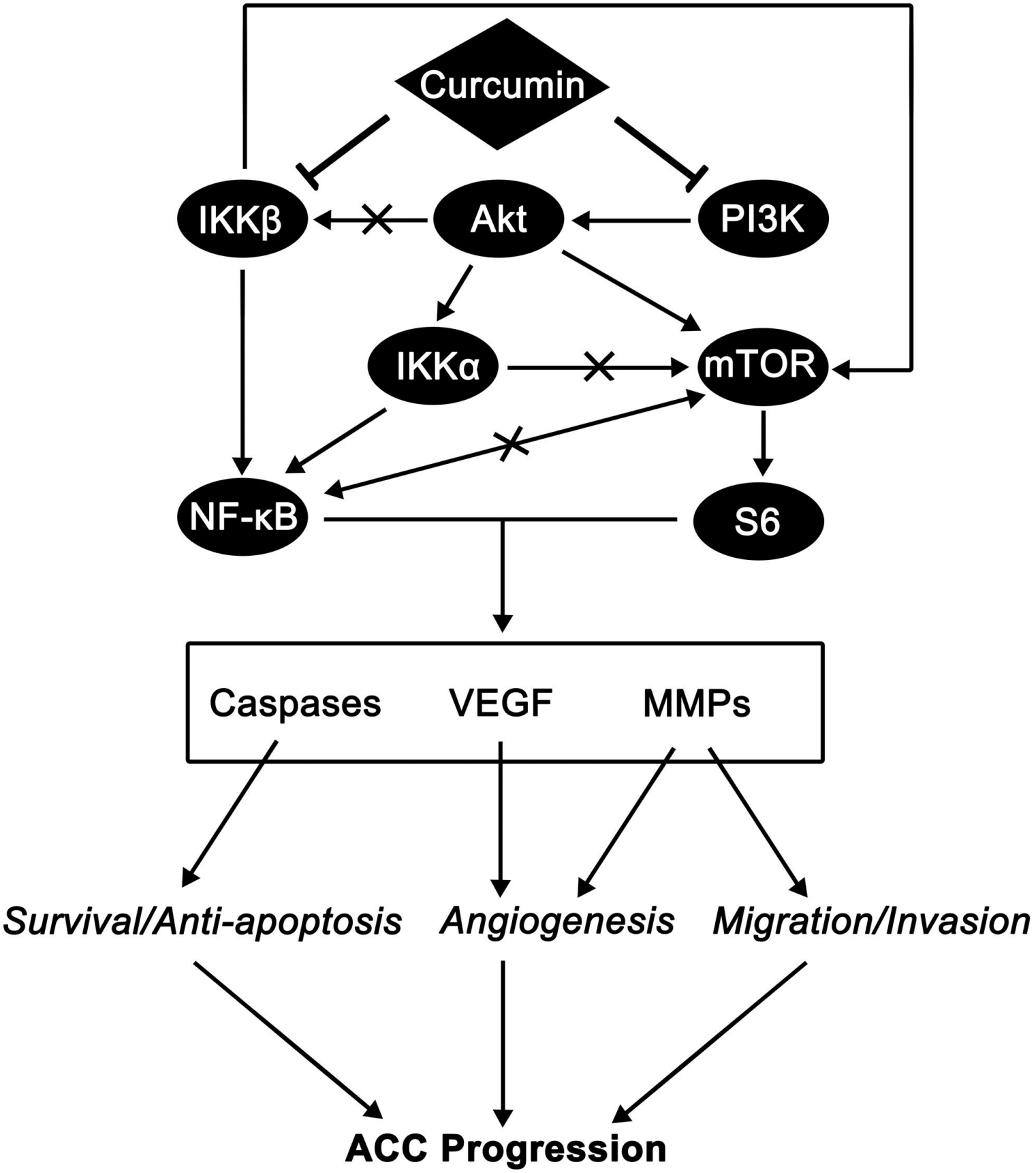
Curcumin
IKKβ
Akt
PI3K
IKKα
mTOR
NF-κB
S6
Caspases
VEGF
MMPs
Survival/Anti-apoptosis
Angiogenesis
Migration/Invasion
ACC Progression

Supplementary data

Molecular Pharmacology #66910

Curcumin dually inhibits both mTOR and NF-κB pathways through a crossed PI3K/Akt/IKK signaling axis in adenoid cystic carcinoma

Zhi-Jun Sun[1], Gang Chen[1], Wei Zhang, Xiang Hu, Yang Liu, Qian Zhou, Ling-Xing Zhu, and Yi-Fang Zhao

The State Key Laboratory Breeding Base of Basic Science of Stomatology & Key Laboratory of Oral Biomedicine Ministry of Education (Z.-J.S., G.C., W.Z., X.H., Y.L., Q.Z., L.-X.Z., Y.-F.Z.); and Department of Oral and Maxillofacial Surgery, School & Hospital of Stomatology, Wuhan University, Wuhan, China (Z.-J.S., G.C., W.Z., X.H., Y.-F.Z.)

Supplementary Materials and Methods

Immunohistochemistry. Paraffin embedded specimens were serially cut into 4-μm sections, deparafinized, and antigen retrieved by microwave. After that, the sections were washed with phosphate-buffered saline (PBS) and incubated within 3% hydrogen peroxide and 10% goat or rabbit serum for 15 min, followed by an overnight incubation with the indicated antibodies (p-mTOR [1:200]; p-S6 [1:200]; NF-κB p65 [1:500]). The antibody binding was detected by horseradish peroxidase-conjugated secondary antibody using diaminobenzidine substrate kit (Dako, Carpinteria, CA) according to the manufacturer's protocol. For analysis, at least five fields with typical pathological changes were randomly selected at a magnification of 400 with light microscope (Leica, Wetzlar, Germany) and counted by two independent observers (ZJ Sun and G Chen) blindly. For NF-κB p65, the staining was localized within both the cytoplasm and/or nucleus, but only the nuclear location of NF-κB p65 was categorized as positive. The rate of the nuclear localization of p65 was calculated as described by Nakayama et al. (Nakayama et al., 2001). For p-mTOR and its downstream target p-S6, the staining scores were calculated as the summation of staining intensity (0, no staining; 1, mild staining; 2, moderate staining; and 3, intense staining) and the percentage of positive cells (0, <10%; 1, 10%-25%; 2, 25%-50%; 3, 50-75%; and 4, 75-100% of stained cells).

Double-Labeling Immunofluorescence Histochemistry. Double-labeling immunofluorescence histochemistry was performed on formalin-fixed, paraffin-embedded 5-μm sections. Briefly, the tissue sections were dewaxed in xylene, hydrated through graded alcohols and distilled water, and washed thoroughly with PBS. Antigen retrieval was done

using 10 mM citrate buffer (pH 6.0) in a pressure cooker heated by microwave oven (80% power) for 20 min. The sections were allowed to cool down and rinsed twice with PBS, and then incubated in 3% hydrogen peroxide in PBS for 30 min, followed by another incubation in 10% nonimmune donkey serum (Sigma-Aldrich, St. Louis, MO) for 1 h at room temperature. After that, excess solution was discarded and the sections incubated with p-S6 (1:100) and p65 (1:100) antibodies together overnight at 4 °C. After washing with PBS, the sections were sequentially incubated with FITC-conjugated donkey anti-rabbit antibody and TRTIC-conjugated donkey anti-mouse antibody (1:200; Jackson ImmunoResearch Laboratories, West Grove, PA), respectively, for 1 h. Nuclei were counterstained with 4,6-diamidino-2-phenylindole (DAPI), followed by observation under a fluorescence microscope.

Hoechst Staining for Morphological Evaluation. ACC-2 and ACC-M cells were seeded on 6-cm culture dishes. After incubation with or without curcumin (20 μM) for 24 h, cells were processed for Hoechst staining. Briefly, cells were fixed in 70% ethanol, washed with PBS, and stained with Hoechst 33258 dye, followed by extensive washes. Nuclear staining was examined under a fluorescence microscopeand three images for each dish were captured using Image-Pro Plus version 5.1 software (Media Cybernetics, Bethesda, MD).

DNA Fragmentation Assay. Induction of apoptosis by curcumin in human ACC cells was assessed by analysis of cytoplasmic histone-associated DNA fragmentation. Briefly, ACC-2 and ACC-M cells at 1×10^4/well were plated in 96-well plates and incubated with or without curcumin for 24 h. Then cytoplasmic histone-associated DNA fragmentation was determined

with the Cell Death Detection ELISA^{PLUS} kit (Roche, Applied Science, Germany) according to the manufacturer's instructions.

Annexin V-FITC/PI Double-Labeling. The quantitative assessment of apoptosis was determined by Annexin V-FITC and PI double-staining flow cytometry. Briefly, ACC-M cells at 1×10^6/well were plated in a 6-cm dish and incubated with or without curcumin for 24 h, then harvested and collected by centrifugation, resuspended in binding buffer, and labeled with Annexin V-FITC and PI double staining kit (BD Biosciences, San Jose, CA) according to the instructions of manufacturer. After incubation in the dark for 30 min, cells were analyzed on the flow cytometer using Cell Quest software. The Annexin V-FITC$^-$/PI$^-$ population was regarded as normal healthy cells, while Annexin V-FITC$^+$/PI$^-$ cells were taken as a measure of early apoptosis, Annexin V-FITC$^+$/PI$^+$ as late apoptosis, and Annexin V-FITC$^-$/PI$^+$ as necrosis.

Caspase Activity Measurement. ACC-M cells at 1×10^6/well were seeded in six-well plates, either untreated or treated with curcumin for 24 h, and then the activities of caspase-9 and -3 were studied. This caspase assay is based on the ability of the active enzyme to cleave the chromophore from the enzyme substrate of caspase-9 (Ac-LEHD-pNA), and caspase-3 (Ac-DEVD-pNA). Briefly, cells were collected, washed with PBS and lysed in lysis buffer for 20 min at 4 °C followed by centrifugation at 10000 × g for 30 min. Then cell lysates were incubated with enzyme specific colorigenic substrates in assay buffer for 2 h at 37 °C. The activity of caspase-9 and -3 was described as the cleavage of colorimetric substrate by measuring the absorbance at 405 nm.

Wound Healing Assay. For determination of cell motility, ACC-M cells (1×10^5 cells/well) were plated in 6-well culture plates and were grown to 80–90% confluence. The center of the cell monolayers were scraped with a sterile micropipette tip to create a gap of constant width. Then the cellular debris was subsequently washed with PBS, and the remaining ACC-M cells were exposed to various concentrations of curcumin as indicated for 12 h. The cells were fixed and stained with acridine orange. Three random images were obtained using a fluorescent microscope with a Leica camera.

Endothelial Cell Migration Assay. To investigate the effects of curcumin on ACC-induced migration of EAhy926 cells, the Transwell Boyden chamber assay was performed as described above. Briefly, conditional medium (CM) from ACC cells pretreated with or without curcumin for 12 h were added to the lower chambers, and then EAhy926 cells were suspended in 100 μL of serum-deprived DMEM medium and seeded into the upper chambers. After 12 h of incubation at 37 °C, migrated cells were fixed with methanol, stained with crystal violet, and then photographed and analyzed.

Capillary-Like Tube Formation Assay. Capillary-like tube formation assay was also performed to examine the effects of curcumin on ACC-induced angiogenesis *in vitro*. EAhy926 cells (2×10^5 cell/dish) in CM from ACC-M cells pretreated with or without curcumin for 12 h were seeded into 6 cm culture dishes coated with Matrigel and incubated for 24 h at 37 °C. After that, the formation of capillary-like structures were observed and captured, the tubes were scanned and quantitated using Image-Pro Plus 5.2 (Media Cybernetics).

Rat Aortic Ring Assay. The thoracic aortas were harvested from Sprague Dawley rats (6 weeks of age) and placed in the 48-well plates coated with 120 μL of Matrigel and sealed in place with an overlay of 50 μL of Matrigel. CM from ACC-M cells pretreated with or without curcumin for 12 h was added to the wells in a final volume of 200 μL. As control, medium alone was assayed. On Day 6, the microvessel outgrowth area was photographed under a phase microscope, and measured with Image-Pro Plus (Media Cybernetics).

Chicken Chorioallantoic Membrane assay. To further investigate the effect of curcumin on tumor-induced angiogenesis, a modified chick chorioallantoic membrane (CAM) assay was carried out. Fertilized White Leghorn chicken eggs were incubated at 37 °C under conditions of constant humidity. The developing CAM was separated from the shell by opening a window at the broad end of the egg above the air sac on Day 7. The opening was sealed with Micropore surgical tape (3M Health Care), and the eggs were returned to the incubator. On Day 9, tape was removed, and sterile filter paper discs containing 20 μL CM were placed on the surface of each CAM. The holes were covered with Micropore surgical tape again and the eggs were incubated for an additional 3 days. The area around the filter paper discs was photographed with a stereo-microscope, and the newly formed vessels were counted in a double-blind manner. Assays for each test sample were carried out using 8-10 eggs.

***In Vivo* Matrigel Plug Assay.** Briefly, 0.6 mL Matrigel containing 0.2 mL CM was injected subcutaneously into nude mice. After 7 days, the skin of the mouse was pulled back to expose the Matrigel plug completely. The plugs were photographed and then hemoglobin was measured using the Drabkin method and Drabkin reagent kit 525 (Sigma-Aldrich).

Semi-Quantitative Reverse Transcription-PCR. The primer sequences for PCR were designed as follows: VEGF: 5'-TCATCTCTCCTATGTGCTGGC-3' and 5'-ATGAACTTTCTGCTCTCTGG-3'; b-FGF: 5'-GTGTGTGCTAACCGTTACCT-3' and 5'-GCTCTTAGCAGACATTGGAAG-3'; G-CSF: 5'-AGACAGGGAAGAGCAGAACGG-3' and 5'-GCCAGAGTGAGGGGTGCAA-3'; PDGF: 5'-CCCCTGCCCATTCGGAGGAAGAG-3' and 5'-TTGGCCACCTTGACGCTGCGGTG-3'; MMP-2: 5'-ACTGAGTGGCCGTGTTTGC-3' and 5'-CGCTTCTGGCTGGGTCTGT-3'; MMP-9: 5'-CCTGGAACTCACACGACATCTTC-3' and 5'-TGGAAACTCACACGCCAGAA-3'; IL-6: 5'-TTCAATGAGGAGACTTGCCTG-3' and 5'-ACAACAACAATCTGAGGTGCC-3'; GAPDH (control): 5'-AACGGATTTGGTCGTATTGGG-3' and 5'-CAGGGGTGCTAAGCAGTTGG-3'.

In situ **Detection of Apoptotic Index in Xenografts Tumor Samples.** Apoptotic cells in tumor samples were determined by the terminal deoxynucleotidyl transferase-mediated dUTP-biotin nick end labeling (TUNEL) assay using the *In Situ* Cell Death Detection Kit (Roche) according to the manual. Six representative areas of each section without necrosis were selected and both apoptotic cells and total nuclei cells were counted under a light microscope at ×400 magnification. The apoptotic index was expressed as the percentage of positive apoptotic tumor cells to total tumor cells.

Microvessel Density in Xenografts Tumor Samples. To quantify angiogenesis in xenografts tumor samples, microvessels were identified by CD31 immunofluorescence staining as described by Amornphimoltham et al. (Amornphimoltham et al., 2008). The CD31 stained section were observed under a Leica fluorescence microscope, and images were captured

from different areas in each section. Then the images were processed using Image-Pro Plus (Media Cybernetics). The vessel density in each image was estimated by measuring the pixel intensity in each field of view. The vessel density of each group was represented as intensity per pixel. A total of 20 high power fields were examined from three tumors of each group.

References

Amornphimoltham P, Patel V, Leelahavanichkul K, Abraham RT and Gutkind JS (2008) A retroinhibition approach reveals a tumor cell-autonomous response to rapamycin in head and neck cancer. *Cancer Res* **68**:1144-1153.

Nakayama H, Ikebe T, Beppu M and Shirasuna K (2001) High expression levels of nuclear factor kappaB, IkappaB kinase alpha and Akt kinase in squamous cell carcinoma of the oral cavity. *Cancer* **92**:3037-3044.

Supplementary Table

Immunostaining scores for p-mTOR, p-S6, and NF-κB in NSG (N), as well as cribriform (C), tubular (T) and solid (S) ACC tissues.

Histologic type	p-mTOR	p-S6	NF-κB
C (n = 23)	4.74 ± 0.26[a]	4.82 ± 0.24[a]	12.81 ± 1.12[a]
T (n = 18)	4.72 ± 0.33[a]	5.11 ± 0.27[a]	13.89 ± 1.57[a]
S (n = 9)	5.44 ± 0.38[a]	5.78 ± 0.43[a]	19.17 ± 2.18[b]
N (n = 6)	0.83 ± 0.31[b]	1.00 ± 0.26[b]	0.89 ± 0.80[c]

Values are mean ± SE. Within a column, means not sharing a common superscript letter are significantly different ($P < 0.05$).

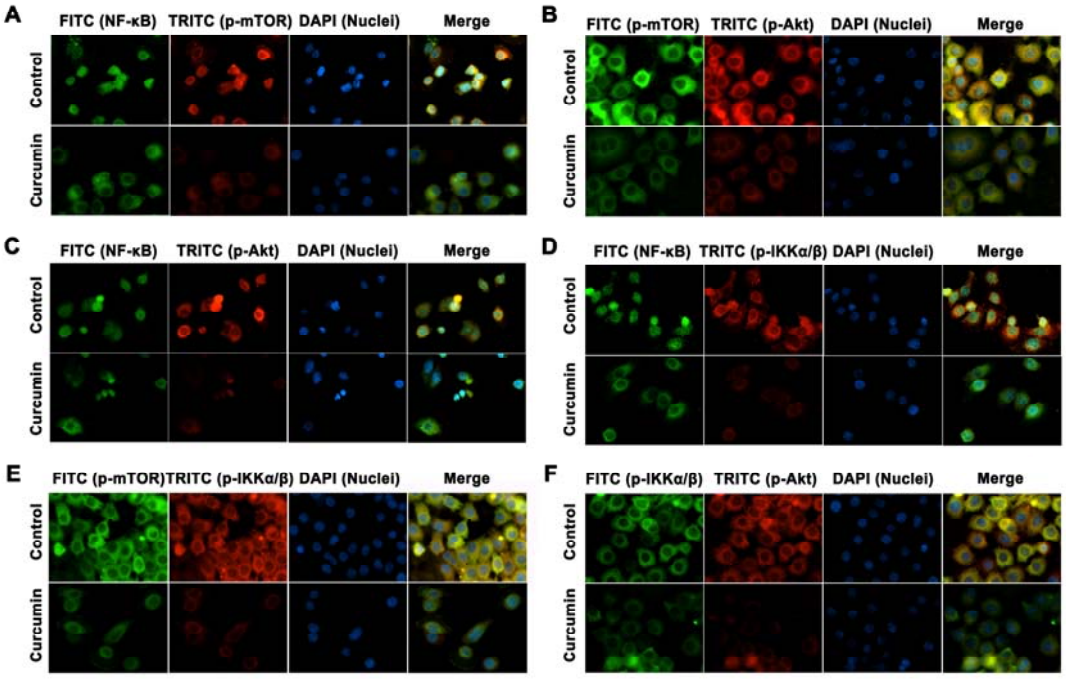

Supplementary Figure 1. Double-labeling immunofluorescence analyses for NF-κB and p-mTOR (A), p-mTOR and p-Akt (B), NF-κB and p-Akt (C), NF-κB and p-IKKα/β (D), p-mTOR and p-IKKα/β (E), as well as p-IKKα/β and p-Akt (F) in ACC-M cells treated with DMSO (Control) or curcumin (20 μM).

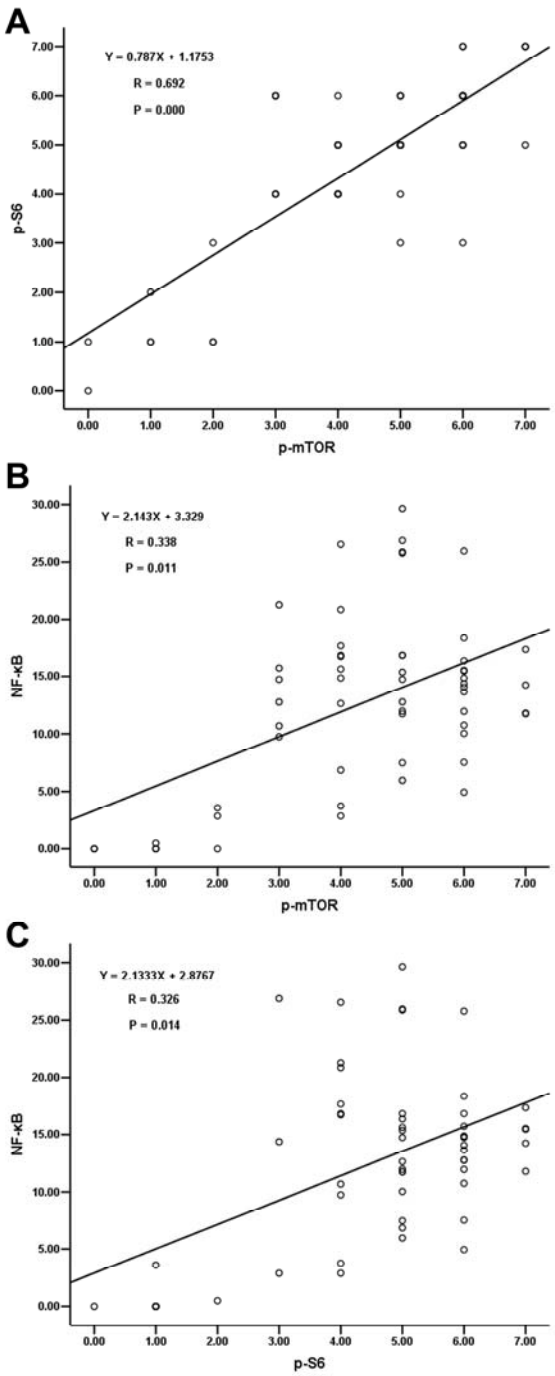

Supplementary Figure 2. Correlation among the activation of mTOR, S6, and NF-κB in ACC tissues. Spearman correlation and linear regression were used to determine the relationship between p-mTOR and p-S6 (A), p-mTOR and NF-κB (B), as well as p-S6 and NF-κB (C), respectively. There were significant correlations among the activation status of mTOR, S6, and NF-κB.

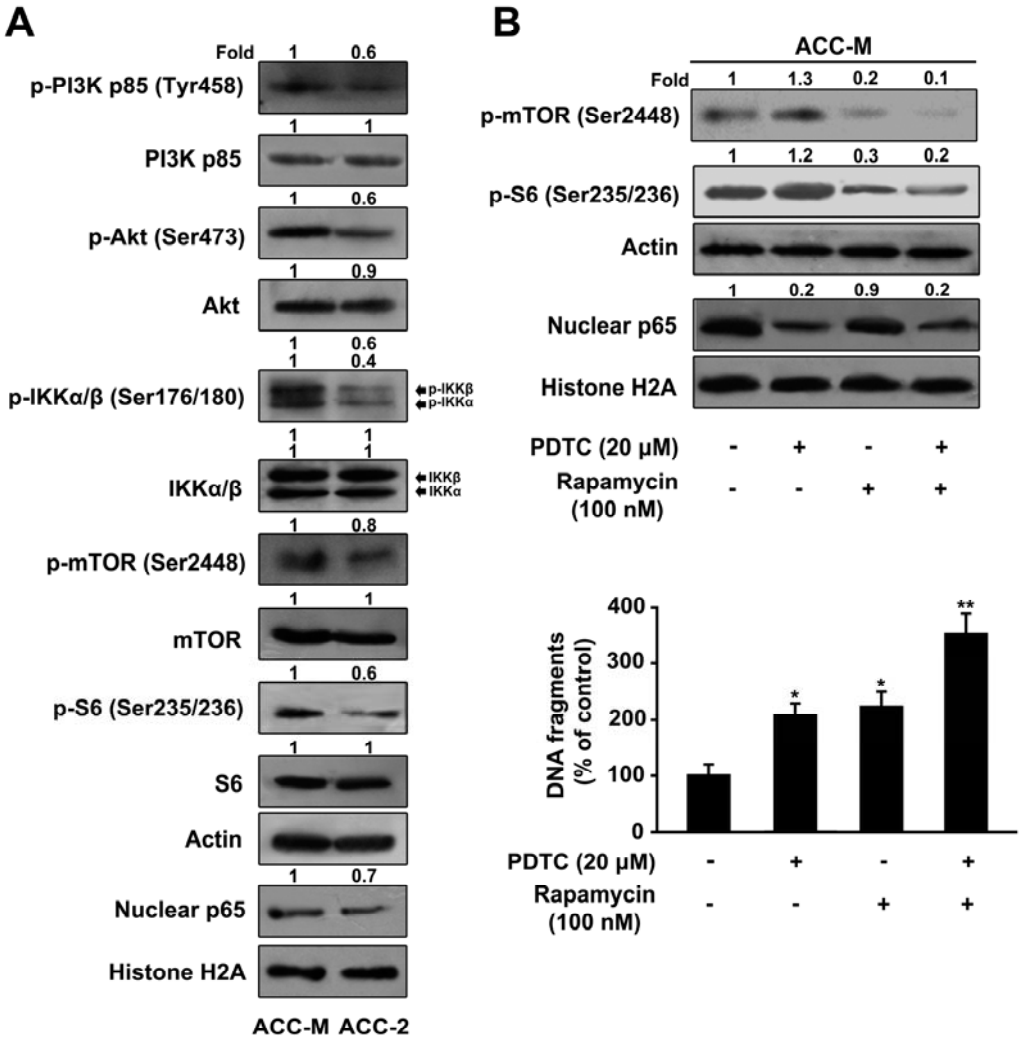

Supplementary Figure 3. Activation status of the NF-κB and mTOR pathways, as well as the PI3K/Akt/IKK signaling axis in ACC cell lines. A, the expression levels of PI3K, Akt, IKKα/β, mTOR, S6 and their phosplorylation forms, as well as nuclear NF-κB were determined by Western blot analysis in ACC-M and ACC-2 cell lines, respectively. B, ACC-M cells were pretreated with PDTC (20 μM) or/and rapamycin (100 nM) for 1 h. The expression levels of p-mTOR, p-S6, as well as nuclear NF-κB were determined by Western blotting. Cell apoptosis was assessed by quantitation of DNA fragmentation using the Cell Death Detection ELISA^{PLUS} assay. All data are presented as mean from three different experiments with duplicate (*, $P < 0.05$; **, $P < 0.01$ versus the control group); bars, ±SE.